Final Report

Project Title Mechanistic Model Incorporating Surface Stress Effects for Analysis of Nanofilms on Surrounding Elastic Medium and Nano-sized Particles Reinforced Composite Materials

By Yasothorn Sapsathiarn

April/2019

สัญญาเลขที่ MRG6080189

รายงานวิจัยฉบับสมบูรณ์

โครงการ แบบจำลองทางกลศาสตร์ที่คำนึงถึงอิทธิพลของหน่วยแรงที่ผิวสำหรับการวิเคราะห์ฟิล์มนาโนบนวัสดุยืดหยุ่นและวัสดุเชิงประกอบเสริมด้วยอนุภาคนาโน

ผู้วิจัย ยโสธร ทรัพย์เสถียร

สังกัด มหาวิทยาลัยมหิดล

สนับสนุนโดยสำนักงานกองทุนสนับสนุนการวิจัยและต้นสังกัด

(ความเห็นในรายงานนี้เป็นของผู้วิจัย สกว.และต้นสังกัด
ไม่จำเป็นต้องเห็นด้วยเสมอไป)

1. Abstract

Project Code : MRG6080189

Project title: **(Thai)** แบบจำลองทางกลศาสตร์ที่คำนึงถึงอิทธิพลของหน่วยแรงที่ผิวสำหรับการวิเคราะห์ฟิล์มนาโนบนวัสดุยืดหยุ่นและวัสดุเชิงประกอบเสริมด้วยอนุภาคนาโน

(English) Mechanistic Model Incorporating Surface Stress Effects for Analysis of Nanofilms on Surrounding Elastic Medium and Nano-sized Particles Reinforced Composite Materials

Investigator : Yasothorn Sapsathiarn, Mahidol University

E-mail Address : yasothorn.sap@mahidol.ac.th

Project Period : 2 years

Nano-scale materials and nanostructures, such as nanoparticles, nanotubes, nanofilms and nanocomposites, are the key components of nano-scale devices. Mechanics of nanomaterials and structures can be understood by incorporating the effect of surface and interfacial energy. Mechanistic models incorporating surface stress effects are developed in this study and applied to examine the influence of surface free energy on the elastic behavior of nanofilms on surrounding elastic medium and nano-sized particles reinforced composite materials. A set of analytical techniques for stress and displacement fields corresponding to elastic nanolayer based on Love's representation, Hankel and Fourier integral transforms are adopted to derive explicit integral form solutions for nanolayer problems. A new three-dimensional finite element formulation for analysis of nanoparticle-reinforced composites is developed in the present work. The finite element model of nanoparticle-reinforced composites provides an efficient tool to analyze and predict the mechanical response of nanocomposites with practically useful arbitrary shaped nano-scale particles, multiple particles, non-symmetric loading, etc. Selected numerical results are presented to portray the features of the field responses of nanofilm-substrate system and properties of nanocomposite materials.

Keywords: Nanotechnology; Mechanistic model; Nanocomposites; Nanofilms; Surface free energy

2. Introduction to the Research Problem

Structures at a nano-scale level are known to exhibit size-dependent behavior (Miller and Shenoy, 2000; Yakobson, 2003). This is attributed to the fact that atoms near the surfaces of solid experience a different local environment than do atoms in the bulk of a material. As a result, when the dimension of a material or structure approaches the nano-scale, the fraction of energy associated with surface atoms becomes comparable to that in the bulk due to a relatively high surface area to volume ratio and the overall mechanical behavior of the material or structure is thus size-dependent. The excess energy associated with the surface atoms is called surface free energy. Comprehensive literature review on the surface effect and the Gibbsian formulation of the thermodynamics of surfaces can be found in general researches of surface and interface stresses (Shuttleworth, 1950; Orowan, 1970; Murr, 1975; Cammarata, 1994; Cammarata, 1997; Fischer et al., 2008). Investigation of the mechanical behavior of nano-scale structures with surface energy effects is currently a topic of substantial interest. In this regard, experimental techniques, theoretical models and computational tools are being developed to investigate the mechanics of nano-structured materials and nano-scale structural elements such as nanofilms, nanotubes, nanobeams, and nanocomposites.

Many researchers are persuaded to study the mechanical behavior of nano-scale structures and materials. Wong et al. (1997) and Poncharal et al. (1999), for instance, experimentally investigated the elastic bending of SiC nanobeams and carbon nanotubes, respectively, and showed that the bending modulus changes as the diameter of the beam or tubes changes. Cadek et al. (2004) measured the tensile modulus of nanotube reinforced polymer composites. Singh et al. (2002) investigated the toughness of nano-scale particle reinforced composites with varies sizes. Oliver and Pharr (1992) established an improved method for determining the hardness and elastic modulus of materials from nano-indentation load-displacement data. It is generally acknowledged that experimental methods yield results reflecting the real behavior of nano-scale structures. However, the behavior is still found to be highly dependent on experimental environments. Moreover, the experiments are expensive to carry out due to the requirement of sophisticated equipment and high-precision testing procedures. The theoretical study using mathematical simulations has, therefore, become an attractive alternative and has been widely used to develop a fundamental understanding and to further predict the complex phenomena. In addition, upon properly calibrating with the data from

basic experiments, mathematical models are found to be capable of simulating responses under various conditions.

Within the framework of modeling nano-scale behavior of solids, two predominant mathematical models have been commonly employed in the literature, one known as the molecular or atomistic models and the other corresponding to the modified or enhanced continuum-based models. The molecular-based models, while providing more precise response prediction, are highly complex and generally consume tremendous computational resources because billions of atoms at a nano-scale need to be modeled. In contrast, the continuum-based models are less complicated and much more computationally efficient. It was discovered that the behavior of atoms near the surface differs from that in the bulk. Hence, to utilize a continuum-based approach instead of the molecular-based simulation, the model for nano-scale structures must be modified properly by incorporating the influence of the surface effects.

Gurtin-Murdoch model, proposed by Gurtin and Murdoch (1975, 1978) and Gurtin et al. (1998), is a mathematical model that incorporates the effects of surface and interfacial energy into continuum mechanics. A good agreement between solutions based on the Gurtin–Murdoch model and atomistic simulations for nano-scale structures has been reported by various researchers (e.g., Lee and Rudd, 2007; Miller and Shenoy, 2000). Gurtin-Murdoch continuum-based model has been widely used in the study of nano-scale problems. For instance, Lim and He (2004) developed a model based on the Gurtin–Murdoch theory to analyze the deformations of a nanoscale film under bending. Lu et al. (2006) generalized the thin plate model to include the normal stresses in the bulk and presented a modified theory for thin and thick plates. It is noted that both studies considered only a special case of one dimensional bending of nano-scale plates. Recently, the nano-scale model and finite element solution for circular nanoplates have been developed by Liu and Rajapakse (2013) and Sapsathiarn and Rajapakse (2013). More recently, Sapsathiarn and Rajapakse (2016, 2018) developed mechanistic models for examined size-dependent responses of nanoscale plates and beams by using Gurtin-Murdoch continuum-based model incorporating surface energy.

Elastic materials containing voids, reinforced-particle and eigenstrain regions are commonly referred as inhomogeneity problems in mechanics literature. Inhomogeneity problems have been studied extensively for several decades since the research work of Eshelby (1957). The books by Nemat-Nasser and Hori (1999) and Marko and Preziosi (2000) have provided comprehensive reviews of the micromechanics of heterogeneous materials. These references deal exclusively

with the classical inhomogeneity problems based on continuum mechanics. With the advantage of nanotechnology, reinforced particles for composite materials can be fabricated with dimensions of the nano-scale. It is well recognized that nano-scale inhomogeneities in a composite can significantly influence the properties of a composite material. Experimental and theoretical researches on modern inhomogeneity problems are required to examine properties and behavior of this class of composite materials. Sharma and Ganti (2004) studied Eshelby's tensor of a nanoinhomogeneity undergoing a dilatational eigenstrain and pointed out that only inhomogeneities with a constant curvature admit a uniform elastic state. Duan et al. (2005) extended the Eshelby formalism for a nano-scale inhomogeneity subjected to an arbitrary uniform eigenstrain. Tian and Rajapakse (2007) obtained a closed-form analytical solution for a nanoscale circular inhomogeneity in an infinite matrix under arbitrary remote loading based on the Gurtin–Murdoch model. Mogilevskaya et al. (2008) and Jammes et al. (2009) examined the elastic interaction problems of multiple inhomogenities in an infinite medium.

An interesting class of problems in thin film/substrate systems deals with the contact mechanics of a surface-loaded layer bonded to an underlying base, which has a wide range of practical applications in the mechanics of microelectronics devices, nanoindentation, and surface coatings. Poulos (1967) solved the plane problem for a vertically loaded strip and presented the stresses and displacements in an elastic layer underlain by a rough rigid base. Lucus et al. (2004) conducted multidimensional nano-contact mechanics experiments for the measurement of both the normal and tangential contact stiffness of film/substrate systems. Gao et al. (2008) gave an analytical formulation to predict the effective elastic modulus of film-on-substrate systems under normal and tangential contact. Nowadays, a film can be fabricated as thin as few nanometers by taking advantage of modern processing technologies. Due to the high ratio of surface to volume of nanofilms, it is necessary to consider the surface energy effect, which is usually neglected in classical mechanics.

On the basis of an extensive literature review, it is found that nano-scale materials and structures have attracted significant interest due to their potential use in the development of nano-devices and advanced materials based on nanotechnology. Current understanding of mechanics of nano-scale materials and structures is very limited. Mechanical responses of nano-scale materials and structures are needed to be examined in order to clearly understand their complex size-dependent behavior. The study of nano-scale inhomogeneity problems has important implications in the development of nanomaterials with superior

properties. The development of the nanofilm-elastic medium system solutions based on the Gurtin-Murdoch theory of elasticity accounting for the surface energy effects is important to the study of the mechanics of nanoindentation, nanofilms and nanocoatings. In addition, this class of problems dealing with a continuum with surface energy effects also has applications in the study of very soft materials such as biological materials and polymer gels and their surface effects. To address these research issues, mechanistic models incorporating surface stress effects for nano-sized particles reinforced composite materials and nanofilm-elastic medium systems are considered in the present research project. A new three-dimensional finite element method (FEM) is to be developed for the analysis of nano-sized particles reinforced composites. The influence of surface stress effects, reinforcement volume fraction, film thicknesses, particle sizes and properties of matrix materials are proposed to investigate. The findings of this project will provide an insight into the complex size-dependent behavior of nanocomposite and nanofilm-elastic substrate system which is essential for the development of nano-scale devices and applications.

3. Objectives of the Research Project

The objectives of the research project are:

1) To develop a three-dimensional finite-element based mechanistic models incorporating surface effects based on Gurtin-Murdoch continuum theory for analysis of nano-sized particles reinforced composite materials for investigating the size-dependent responses of nano-sized particle reinforced composite materials.

2) To develop mechanistic models incorporating surface effects based on Gurtin-Murdoch continuum theory for analysis of nanofilm-elastic medium system and investigate the influence of various parameters on the response of nanofilm-elastic medium system.

4. Research Methodology, Results and Discussion

The present research project is concerned with the development of mechanistic models incorporating surface stress effects for the analysis of nanofilm-elastic medium system and nano-sized particles reinforced composite materials. The research methodology, procedures and fundamental theories to be employed in the research project are summarized as follows:

4.1 Surface elasticity model

In order to incorporate the surface stress effects for the elastic fields of nanocomposites and nanofilms-elastic medium systems, an extra group of basic equations is needed in addition to those of classical elasticity. Models of nanofilms and nano-sized particles based on the Gurtin-Murdoch continuum theory have an elastic surface, mathematically zero thickness, perfectly bonded to the bulk material. The elastic surface has distinct material properties and accounts for the surface energy effects (Miller and Shenoy, 2000; Lee and Rudd, 2007). In Gurtin–Murdoch model, a linearized surface stress–strain constitutive relation is proposed to characterize the surface/interface stress effect. The equilibrium and constitutive equations of the bulk solid are the same as those in the classical elasticity, but the presence of surface/interface stress gives rise to non-classical boundary conditions. The generalized Young-Laplace equation (Povstenko, 1993), surface constitutive relations and strain-displacement relationship of the surface can be expressed as (Gurtin and Murdoch, 1975; Gurtin and Murdoch, 1978)

$$\sigma^s_{\beta\alpha,\beta} + \sigma_{\beta\alpha} n_\beta = 0; \;\; \sigma_{ji} n_i n_j = \sigma^s_{\beta\alpha} k_{\beta\alpha} \tag{1}$$

$$\sigma^s_{\beta\alpha} = \tau_0 \delta_{\beta\alpha} + 2\left(\mu_0 - \tau_0\right)\varepsilon_{\beta\alpha} + \left(\lambda_0 + \tau_0\right)\varepsilon_{\gamma\gamma}\delta_{\beta\alpha} + \tau_0 u^s_{\beta,\alpha} \tag{2}$$

$$\varepsilon^s_{\alpha\beta} = \frac{1}{2}\left(u^s_{\alpha,\beta} + u^s_{\beta,\alpha}\right) \tag{3}$$

where μ_0 and λ_0 are surface Lamé constants; τ_0 is the residual surface tension under unstrained conditions; the superscript ‘s’ denotes the quantities corresponding to the surface; n_i denotes the components of the unit normal vector of the surface; and $k_{\beta\alpha}$ is the curvature tensor of the surface. It should be noted that the surface stress tensor is a 2D quantity. The Greek indices take the value of 1 or 2, while Latin subscripts adopt values from 1 to 3. The surface material properties, μ_0, λ_0 and τ_0 can be determined from atomistic simulations (Shenoy, 2005).

4.2 Nano-sized particle reinforced composite materials

Consider a composite of elastic matrix material containing a nanoscale inhomogeneity as shown in Figure 1. The Cartesian coordinate system is used in the formulation. The matrix and inhomogeneities have no body force and are linearly elastic, homogenous and anisotropic. The inhomogeneities can be arbitrary shaped and in the nanometer range. The bonding between matrix and inhomogeneity is assumed to be perfect. The composite material system is subjected to external loads on the outer surface S of the matrix material. The Gurtin-Murdoch continuum theory

(1975, 1978) accounting for surface energy effects due to the presence of nanoscale inhomogeneities is considered in the formulation by adding the surface layer Γ to the nanoscale inhomogeneities.

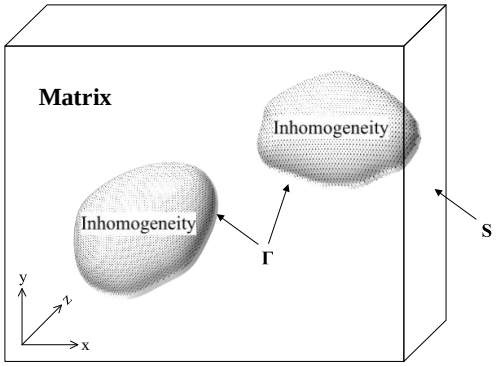

Figure 1 Nanoscale inhomogeneities in an elastic matrix.

The classical finite element formulation (Zienkiewicz and Taylor, 2000) is extended to formulate the problem of composite material containing nanoscale inhomogeneities. The surface stress effect based on Gurtin is also implemented in the finite element formulation. The potential energy approach is used to develop the finite element equations. The finite element formulation developed in the present study can be used to solve complicated nanoscale mechanics problems such as arbitrary shaped inhomogeneities, anisotropic matrix and inhomogeneity materials, and unit cells containing nanoscale inhomogeneity.

The total potential energy of the system (Π) as shown in Figure 1 can be obtained by the summation of the strain energy of the bulk material (U^B), the strain energy of the surface/interface (U^S) and the work by external force (W) as

$$\Pi = U^B + U^S + W \tag{4}$$

The strain energy of the bulk material is given by,

$$U^B = \int_{V_I} \int_0^{\varepsilon_{ij}} \sigma_{ij}^B d\varepsilon_{ij} dV + \int_{V_M} \int_0^{\varepsilon_{ij}} \sigma_{ij}^B d\varepsilon_{ij} dV \tag{5}$$

and the work done by external body force $\{b\}$ and surface traction $\{t\}$ is given by,

$$W = -\iiint_V \frac{1}{2}\{u\}^{\mathrm{T}}\{b\}\,dV - \int_{\Gamma_M} \{u\}^{\mathrm{T}}\{t\} d\Gamma \tag{6}$$

in which the superscript B denotes quantities corresponding to the bulk for both of the matrix and inhomogeneities; the volume of the matrix and inhomogeneities are

denoted as V_M and V_I respectively; the vector $\{t\}$ is the surface traction vector due to applied load, and the surface displacement vector is denoted as $\{u\}$; the superscript T denotes the transport of the vector and matrix.

The strain energy of the the surface/interface with surface stress constitutive relationship is given by,

$$U^S = \int_{\Gamma_I+\Gamma_M} \{\varepsilon\}^{\mathrm{T}} \left[D^S\right] \{\varepsilon\} d\Gamma \tag{7}$$

where Γ_M and Γ_I denote the boundary surface of the matrix and the matrix-particle interface, respectively; the superscript S denotes quantities corresponding to the surface and the integral with respect to $d\Gamma$ is taken over the matrix-inhomogeneity interface and the boundary surface of the matrix.

The element shape function matrix $\left[N(x,y)\right]$ can be introduced by

$$u = N \bar{u} , \tag{8}$$

where $\{u\}$ is the displacement vector at a general point within an element, and $\{\bar{u}\}$ is the nodal displacement vector.

For a three-dimensional problem, these two displacement vectors can be written as,

$$u = u_x, u_y, u_z \quad^T \tag{9a}$$

$$\bar{u} = \bar{u}_{x\,1}\ \bar{u}_{y\,1}\ \bar{u}_{z\,1}\ \bar{u}_{x\,2}\ \bar{u}_{y\,2}\ \bar{u}_{z\,2} \cdots \bar{u}_{x\,n}\ \bar{u}_{y\,n}\ \bar{u}_{z\,n}\quad^T \tag{9b}$$

where the subscript '*n*' denote number of node in the element.

Differentiating Eq. (8) with respect to the coordinates, the corresponding element strain vector can be expressed as,

$$\{\varepsilon\} = \frac{\partial\{u\}}{\partial x_i} = \left[\frac{\partial[N]}{\partial x_i}\right]\{\bar{u}\} = [B]\{\bar{u}\}, \tag{10}$$

where [*B*] is a matrix including derivatives of the element shape function.

Integrating Eq. (5) with respect to the strains and using linear stress-strain relation for the matrix and inhomogeneity materials result in,

$$U^B = \int_{V_M} \frac{1}{2}\{\varepsilon\}^T [D]_M \{\varepsilon\} dV + \int_{V_I} \frac{1}{2}\{\varepsilon\}^T [D]_I \{\varepsilon\} dV \tag{11}$$

where $[D]_M$ and $[D]_{\mathrm{M}}$ are the 3-D elasticity matrices of the matrix and inhomogeneity materials respectively.

Substitution of Eq. (8) into (6) yields,

$$W = -\int_S \left([N]\{u\}^T \right)\{T\}\, dS = -\int_S \{[\bar{u}]\}^T \left([N]\right)^T \{T\}\, dS \tag{12}$$

The surface elastic stain energy due to surface stress component can be expressed as,

$$U^S = \int_{\Gamma+S} \frac{1}{2}\ \varepsilon^{\ T}\ D_{\ S}\ \ \varepsilon\ \ d\Gamma \tag{13}$$

Using Eqs. (11), (12), and (13), and the strain-displacement relation, the potential energy functional can be expressed as,

$$\Pi = \int_{V_M} \frac{1}{2}\ \bar{u}^{\ T}\ B^T\ D_{\ M}\ B\ \ \bar{u}\ \ dV + \int_{V_I} \frac{1}{2}\ \bar{u}^{\ T}\ B^T\ D_{\ I}\ B\ \ \bar{u}\ \ dV$$

$$-\int_S N\ \ \bar{u}^{\ T}\ \ T\ \ dS + \int_{\Gamma+S} \frac{1}{2}\ \bar{u}^{\ T}\ B^T\ D_{\ S}\ B\ \ \bar{u}\ \ d\Gamma \tag{14}$$

Now apply the stationary condition of Π, i.e., $\delta\Pi = 0$, with respect to the unknow nodal displacement vector. In view of Eq. (14), the variation of the each energy term in Π can be expressed as,

$$\delta U^B = \ \delta\bar{u}^{\ T}\left(\int_{V_M} B^T\ D_{\ M}\ B\ dV\right)\ \bar{u}\ +\ \delta\bar{u}^{\ T}\left(\int_{V_I} B^T\ D_{\ I}\ B\ dV\right)\ \bar{u}$$

$$-\ \delta\bar{u}^{\ T}\left(\int_I B^T\ D_{\ I}\ B\ dV\right) \tag{15a}$$

$$\delta W = -\ \delta\bar{u}^{\ T}\int_S N^{\ T}\ T\ \ dV, \tag{15b}$$

$$\delta U^S = \{\delta\bar{u}\}^T\left(\int_{\Gamma+S} [B]^T\left[\bar{D}\right]_S \{\varepsilon\}\, d\Gamma\right) \tag{15c}$$

Finally, the equilibrium equation can be expressed as,

$$K\ \ \bar{u}\ =\ f \tag{16a}$$

in which

$$K = \int_{V_M} B^T D_M B \, dV + \int_{V_I} B^T D_I B \, dV$$

$$+ \int_{\Gamma+S} B^T D_S B \, d\Gamma \tag{16b}$$

$$\{f\} = \int_S [N]\{T\} dS \tag{16c}$$

A micromechanical model based on finite element formulation is also developed in the present work for the study of elastic materials containing nanoscale inhomogeneities. The micromechanical analysis is performed by using a micromechanics theory which relates mechanics between two different length scale problems, i.e., (1) the macroscopic level in which the material is conceptually represented as a homogeneous material and (2) the level of the constituents in which the material properties are always heterogeneous and consist of distinguishable phases such as the main matrix material, inclusions and cavities or voids. Properties of elastic materials containing nanoscale inhomogeneities can be determined by the analysis in the level of the constituents. The analysis might be performed on a "representative volume element" or a "unit cell" which can be isolated from the composite material and is in a state of equilibrium. The unit cell for materials considered in the present work is schematically presented in Figure 2.

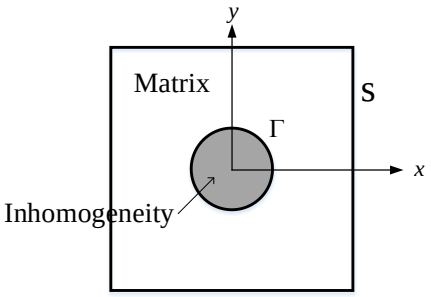

Figure 2 A unit cell for composite materials containing a nanoscale inhomogeneity, e.g., nanovoid or nanoparticle.

The macroscopic constitutive relation of the materials with nanoscale inhomogeneities can be expressed in terms of the macro stress and the macro strain as

$$\{\bar{\sigma}\} = \left[C^{eff}\right]\{\bar{\varepsilon}\} \tag{17}$$

where

$$\{\bar{\sigma}\} = \begin{matrix} \bar{\sigma}_{xx} & \bar{\sigma}_{yy} & \bar{\sigma}_{xy} \end{matrix}^{\mathrm{T}} \tag{18a}$$

$$\left[C^{eff}\right] = \begin{bmatrix} C_{11}^{eff} & C_{12}^{eff} & 0 \\ C_{12}^{eff} & C_{22}^{eff} & 0 \\ 0 & 0 & C_{66}^{eff} \end{bmatrix} \tag{18b}$$

According to the micromechanics theory, the macro stress, $\bar{\sigma}_{ij}$, and macro strain, $\bar{\varepsilon}_{ij}$, can be defined as the volume average stress in a representative volume element as

$$\bar{\sigma}_{ij} = \frac{1}{V}\int_{\Omega} \sigma_{ij}\, d\Omega \tag{19a}$$

$$\bar{\varepsilon}_{ij} = \frac{1}{V}\int_{\Omega} \varepsilon_{ij}\, d\Omega \tag{19b}$$

A selected set of numerical solutions is presented for the plane strain case of elastic material with nanoscale inhomogeneity to portray the response within nano-structured materials and investigate the influence of inhomogeneity volume fraction to the mechanical properties of the nano-structured materials. Two types of materials are considered in the numerical simulation, i.e. (1) nanocomposite materials (i.e., materials containing nanoscale particles) and (2) nanoporous materials (i.e., materials containing nanoscale cavities or voids). The matrix and particle inhomogeneity materials are considered to be linearly elastic and isotropic in the numerical study with Lame′ constants, E_M = 40 GPa, v_M = 0.20 GPa for the matrix material and E_I = 80 GPa, v_I = 0.25 GPa for the particle inhomogeneity material. The surface parameter $K^S = 2\mu^S + \lambda^S - \tau_0 = 10$ N/m is considered in the numerical example.

The unit cell subjected to a prescribed displacement in the x-direction over the positive x face (a surface that is perpendicular to the x-axis and on the positive x side) is considered in the numerical example. The other faces are constrained in such a way that only the movement in the x-direction is allowed and the displacements in all other directions are prevented. The properties of nanocomposite and nanoporous materials can be determined from the fields within the unit cell being considered by using Eqs. (17)-(19).

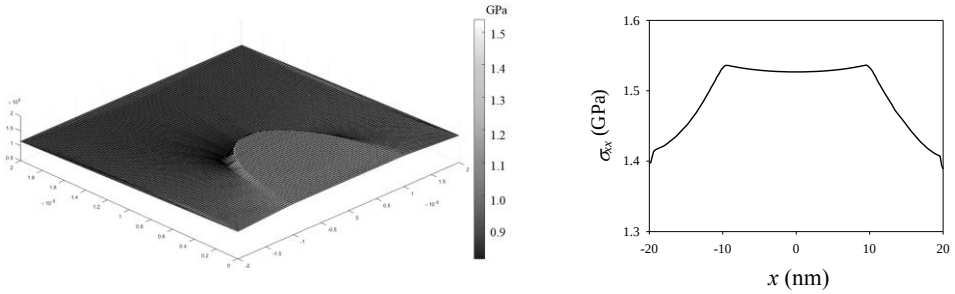

(a) σ_{xx} distribution (b) σ_{xx} profile (across the inhomogeneity)

Figure 3 (a) Distribution and (b) profile of the stress σ_{xx} for nanocomposites with circular nano-particles

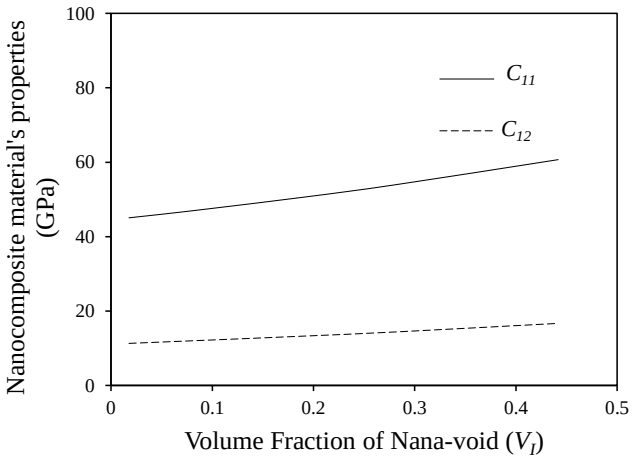

Figure 4 Variation of material properties of nanocomposites with circular nano-particles versus the volume fraction of the inhomogeneity (V_I).

The numerical results for the case of nanocomposites containing circular nano-particles are presented in Figures 3 and 4. The distribution of stress σ_{xx} over the half-domain of the unit cell is presented in Figure 3(a) for a nanocomposite material with volume fraction of the inhomogeneity V_I = 0.2. The corresponding profile of stress σ_{xx} along the x-axis across the center of the nano-particle inhomogeneity is presented in Figure 3(b). The unit cell is stretched and the tensile stress σ_{xx} is generated all over the unit cell. The stress σ_{xx} in the domain of inhomogeneity is generally higher compared to those in the matrix domain showing the stress disturbance in a composite material due to the presence of the nanoscale inhomogeneity. The influence of volume

fraction of the inhomogeneity (V_I) to the mechanical properties C_{11}^{eff} and C_{12}^{eff} of the nanocomposite can be observed in Figure 4. It is shown in Figure 4 that the properties of nanoinclusion material are increasing as the volume fraction c increases. It should be observed that the relations between the material coefficients and V_I are non-linear.

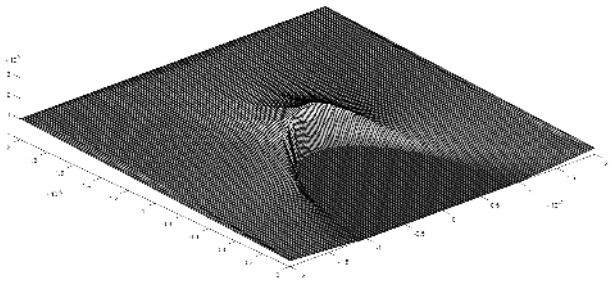

Figure 5 Distribution of the stress σ_{xx} for nanoporous material's properties with circular nano-voids.

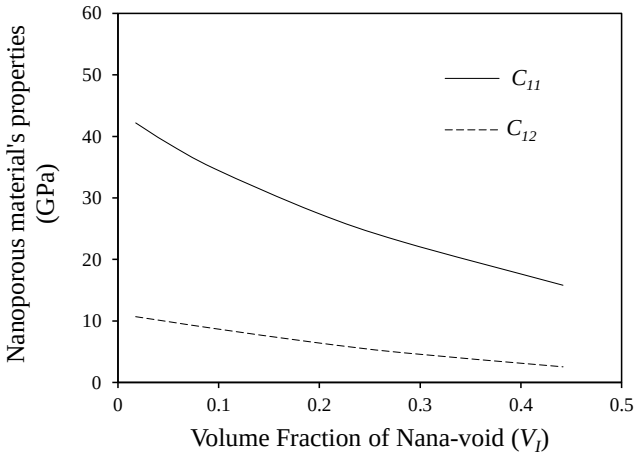

Figure 6 Variation of nanoporous material's properties (circular nano-voids) versus the volume fraction of the inhomogeneity (V_I).

The stress distribution and properties of nanoporous material with circular nano-voids considered in the numerical study are presented in Figures 5 and 6 respectively. The volume fraction of the inhomogeneity (nanoscale voids) considered in Figure 5 is V_I = 0.2. Similar behavior is observed for the case of a nanoporous material, i.e., the unit cell is stretched and the tensile stress σ_{xx} is generated all over the domain. Based on the results shown in Figure 5, the stress concentration in the vicinity of a nanovoid

is noted. Similar to the case of nanocomposite, the dependence of nanoporous material's properties on the volume fraction of the inhomogeneity (V_I) is non-linear (see Figures 3 and 4). As expected, the properties of nanoporous material are decreasing as the volume fraction of nanovoid V_I increases as can be seen in Figure 6.

4.3 Nanofilm-elastic medium systems

Modified continuum models for the analysis of nanofilms resting on Winkler support are presented in this section. Two models of nanofilms are developed in this study, i.e., thin nanoplates and elastic nanolayers. The formulation of both models are based on the Gurtin-Murdoch continuum theory accounting for surface energy. Analytical solutions for circular and rectangular thin nanoplates with all edges simply supported, subjected to vertical load, and rested on Winkler support are presented in the subsequent section. Elastic nanolayer on Winkler support under vertical loadings are formulated for plane strain and axisymmetric cases. A set of analytical techniques for stress and displacement fields corresponding to elastic nanolayer based on Love's representation, Hankel and Fourier integral transforms are adopted to derive explicit integral form solutions for nanolayer problems.

4.3.1 Nano-scale thin plates on Winkler support

First, consider an incremental element of a thin rectangular nanoplate with a Cartesian coordinate system (x, y, z) as shown in Figure 7. It is assumed that the response of the nanofilm is governed by the continuum thin plate theory proposed by Gurtin and Murdoch (1975a, 1975b) and its deflections are small and strains are infinitesimal. The stiffness of the supporting elastic substrate is represented by a Winkler model in which the support reaction is linearly proportional to the nanofilm deflection w by the coefficient k. According to the Gurtin-Murdoch theory (Gurtin and Murdoch, 1975a and 1975b), the plate element consists of a bulk material and surface layer of zero mathematical thickness.

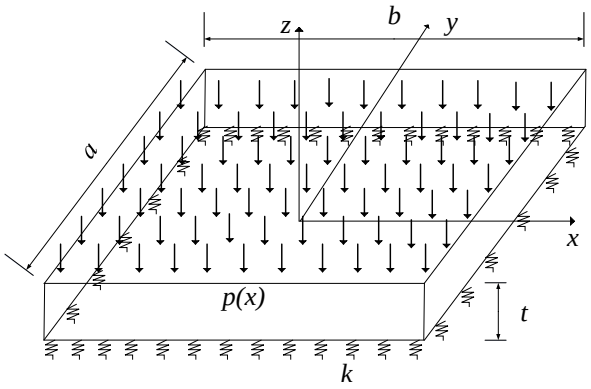

Figure 7 Rectangular nanofilm on Winkler support.

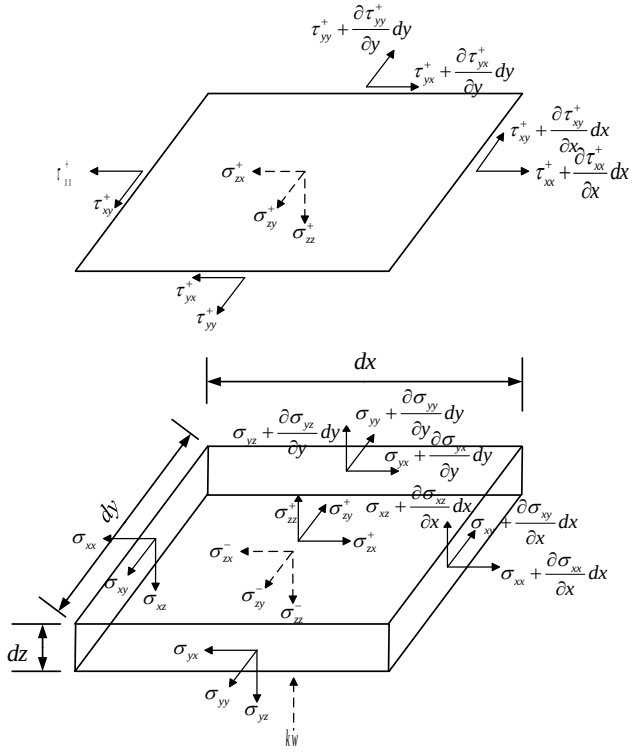

Figure 8 Stress components of an incremental element of the surface layer and bulk element.

The formulation of rectangular nanoplates governing equations has been presented by Sapsathiarn and Rajapakse (2016). The governing Equations of Nanofilm on Winkler Support is considered in the present work. Stresses acting on the surface and bulk incremental elements are shown in Figure 8.

The force equilibrium equations of the top (Figure 7) and bottom surfaces can be expressed as,

$$\tau^{+}_{\alpha i,\alpha} - \sigma^{+}_{zi} = 0, \tag{20a}$$

$$\tau^{-}_{\alpha i,\alpha} - \sigma^{-}_{zi} = 0 \tag{20b}$$

where $\tau^{\pm}_{\alpha i}$ and $\sigma^{\pm}_{zi}$ denote surface stress and the resulting contact tractions, respectively, with superscripts "-" and "+" indicating the components of the bottom and top surfaces, respectively.

The equilibrium of an incremental element of the bulk in the $x-$direction can be expressed as:

$$\int_{-t/2}^{t/2} \frac{\partial \sigma_{xx}}{\partial x} dz + \int_{-t/2}^{t/2} \frac{\partial \sigma_{yx}}{\partial y} dz + \sigma^{+}_{zx} - \sigma^{-}_{zx} + \int_{-t/2}^{t/2} b_x dz = 0 \tag{21}$$

where σ_{ij} and b_i are bulk stresses and body forces respectively; and t is the thickness of the plate.

Similarly, the equilibrium of the bulk element in the y- and z-directions respectively yield,

$$\int_{-t/2}^{t/2} \frac{\partial \sigma_{xy}}{\partial x} dz + \int_{-t/2}^{t/2} \frac{\partial \sigma_{yy}}{\partial y} dz + \sigma^{+}_{zy} - \sigma^{-}_{zy} + \int_{-t/2}^{t/2} b_y dz = 0 \tag{22a}$$

$$\int_{-t/2}^{t/2} \frac{\partial \sigma_{xz}}{\partial x} dz + \int_{-t/2}^{t/2} \frac{\partial \sigma_{yz}}{\partial y} dz + \sigma^{+}_{zz} - \sigma^{-}_{zz} + \int_{-t/2}^{t/2} b_z dz + kw(x,y) - p(x,y) = 0 \tag{22b}$$

where $p(x,y)$ and $w(x,y)$ are applied vertical load and vertical displacement of the plate, respectively.

Next, the moment equilibrium equations of the bulk element about the y- and x-axis can be expressed as:

$$\int_{-t/2}^{t/2} \left(\frac{\partial \sigma_{xx}}{\partial x} + \frac{\partial \sigma_{yx}}{\partial y} \right) z dz + \frac{t}{2}(\sigma^{+}_{zx} - \sigma^{-}_{zx}) - \int_{-t/2}^{t/2} \sigma_{xz} dz + \int_{-t/2}^{t/2} b_x z dz = 0, \tag{23a}$$

and

$$\int_{-t/2}^{t/2} \left(\frac{\partial \sigma_{xy}}{\partial x} + \frac{\partial \sigma_{yy}}{\partial y} \right) z dz + \frac{t}{2}(\sigma^{+}_{zy} - \sigma^{-}_{zy}) - \int_{-t/2}^{t/2} \sigma_{yz} dz + \int_{-t/2}^{t/2} b_y z dz = 0. \tag{23b}$$

Assume that the bulk material is homogeneous and isotropic and let E and ν denote its Young's modulus and Poisson's ratio respectively. Its constitutive

relations can be expressed as,

$$\sigma_{xx} = \frac{E}{1-\nu^2}\varepsilon_{xx} + \frac{E\nu}{1-\nu^2}\varepsilon_{yy} + \frac{\nu}{1-\nu}\sigma_{zz} \tag{24a}$$

$$\sigma_{yy} = \frac{E}{1-\nu^2}\varepsilon_{yy} + \frac{E\nu}{1-\nu^2}\varepsilon_{xx} + \frac{\nu}{1-\nu}\sigma_{zz} \tag{24b}$$

$$\sigma_{i\alpha} = \frac{E}{1-\nu^2}\varepsilon_{i\alpha} \tag{24c}$$

In the present research project, bulk stress σ_{zz} is assumed to vary linearly through the plate thickness to satisfy the equilibrium conditions on the surface. Therefore,

$$\sigma_{zz} = \frac{1}{2}(\sigma_{zz}^{+} + \sigma_{zz}^{-}) + \frac{z}{t}(\sigma_{zz}^{+} + \sigma_{zz}^{-}). \tag{25}$$

Rewriting σ_{zz} in terms of surface stresses using Eq. (2) and assuming $\rho_0^{+} = \rho_0^{-} = \rho_0$ yields,

$$\sigma_{zz} = \frac{1}{2}(\tau_{\alpha z,\alpha}^{+} - \tau_{\alpha z,\alpha}^{-}) + \frac{z}{t}(\tau_{\alpha z,\alpha}^{+} + \tau_{\alpha z,\alpha}^{-}). \tag{26}$$

For a Kirchhoff plate,

$$u_x = -z\frac{\partial w}{\partial x};\ u_y = -z\frac{\partial w}{\partial y};\ u_z = w(x, y) \tag{27}$$

The relevant strain-displacement relations for the bulk materials are,

$$\varepsilon_{xx} = -z\frac{\partial^2 w}{\partial x^2};\ \varepsilon_{yy} = -z\frac{\partial^2 w}{\partial y^2};\ \varepsilon_{xy} = -z\frac{\partial^2 w}{\partial x \partial y} \tag{28}$$

and $\varepsilon_{xz} = \varepsilon_{yz} = \varepsilon_{zz} = 0$.

After further manipulations, the following governing equation for a thin plate incorporating the effects of surface energy can be obtained based on Eqs. (20) - (28).

$$D^{*}\nabla^2\nabla^2 w - 2\tau^{s}\nabla^2 w + kw - p(x) = 0 \tag{29}$$

where $D^* = \frac{Et^3}{12(1-\nu^2)} + \frac{t^2}{2}(2\mu^s + \lambda^s) - \frac{t^2\tau^s\nu}{6(1-\nu)}$ and

$\nabla^2 = \frac{\partial^2}{\partial x^2} + \frac{\partial^2}{\partial y^2}$ for Cartesian coordinate system,

$\nabla^2 = \frac{\partial^2}{\partial r^2} + \frac{1}{r}\frac{\partial}{\partial r} + \frac{\partial^2}{\partial z^2}$ for Cylindrical coordinate system.

Solution of Rectangular Nanofilm on Winkler Support with All Edges Simply Supported (SSSS)

For all edges simply-supported, the boundary conditions are given by

$$w = 0\big|_{x=0,a};\ w = 0\big|_{y=0,b}, \tag{30a}$$

$$M_x^* = 0\big|_{x=0,a};\ M_y^* = 0\big|_{y=0,b} \tag{30b}$$

where $M_x^* = -D^*\frac{\partial^2 w}{\partial x^2} - D_1^*\frac{\partial^2 w}{\partial y^2}$; $M_y^* = -D^*\frac{\partial^2 w}{\partial y^2} - D_1^*\frac{\partial^2 w}{\partial x^2}$ and

$D_1^* = \frac{Et^3\nu}{12(1-\nu^2)} + \frac{t^2}{2}(\lambda^s + \tau^s)$.

The general solution of Eq. (29) can be written in the double Fourier series form as

$$w(x,y) = \sum_{m=1}^{\infty}\sum_{n=1}^{\infty} w_{mn}\sin\frac{m\pi x}{a}\sin\frac{n\pi y}{b} \tag{31}$$

and the distributed loading is represented by

$$p(x,y) = \sum_{m=1}^{\infty}\sum_{n=1}^{\infty} p_{mn}\sin\frac{m\pi x}{a}\sin\frac{n\pi y}{b},\ 0<x<a,\ 0<y<b \tag{32}$$

Substituting Eqs. (31) and (32) into Eq. (29) and equating coefficients, the unknown coefficients in Eq. (29) can be obtained as

$$w_{mn} = \frac{p_{mn}}{D^*\pi^4\left(\frac{m^2}{a^2}+\frac{n^2}{b^2}\right)^2 + 2\tau^s\pi^2\left(\frac{m^2}{a^2}+\frac{n^2}{b^2}\right) + k} \tag{33}$$

in which $p_{mn} = \frac{4p_0}{\pi^2 mn}(1-\cos m\pi)(1-\cos n\pi)$ for a uniformly distributed loading.

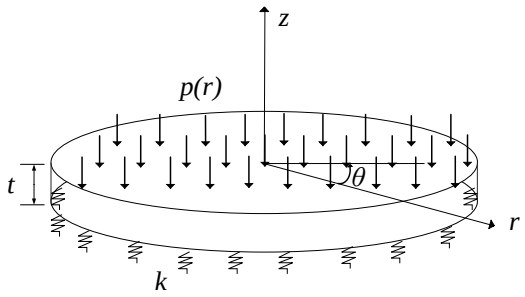

Figure 9 Circular nanofilm on Winkler support.

Solution of Circular Nanofilm on Winkler Support with All Edges Simply Supported (SSSS)

Analytical solution of a circular nanofilm on Winkler support in the cylindrical polar coordinates presented in Figure 9 is now considered. The governing equation for a circular nanofilm on Winkler support can be written as

$$D^*\nabla_2^2\nabla_2^2 w - 2\tau^s\nabla_2^2 w + kw - p(r) = 0 \tag{34}$$

The solution of Eq. (34) under uniformly distributed load p_0 can be obtained as

$$\overline{w}(\overline{r}) = A_1 J_0(\lambda_1\overline{r}) + A_2 Y_0(\lambda_1\overline{r}) + A_3 I_0(\lambda_2\overline{r}) + A_4 K_0(\lambda_2\overline{r}) + \frac{p_0}{kR} \tag{35}$$

where J_0, Y_0, I_0 and K_0 are the Bessel functions of the first and second kind and the modified Bessel functions of the first and second kind, respectively (Sneddon, 1951; Gradshteyn and Ryzhik, 2000); $A_1 - A_4$ are unknown arbitrary functions to be determined and

$$\lambda_1^2 = \frac{-\tau^s + \sqrt{\tau^{s2} + kD^*}}{D^*} R^2 \tag{36a}$$

$$\lambda_2^2 = \frac{\tau^s + \sqrt{\tau^{s2} + kD^*}}{D^*} R^2. \tag{36b}$$

The resultant moment of a cross section is given by

$$M^* = -D^*\frac{d^2 w}{dr^2} - \frac{D_2^*}{r}\frac{dw}{dr} \tag{37}$$

where $D_2^* = \dfrac{Et^3\nu}{12(1-\nu^2)} + \dfrac{t^2(\lambda^s + \tau^s)}{2} - \dfrac{\tau^s\nu t^2}{6(1-\nu)}$.

The boundary conditions for a circular nanofilm with simply supported are

$$\bar{w}(1) = 0,\ M^*(1) = 0 \tag{38}$$

Substituting Eq. (35) into the boundary conditions Eq. (38) and noting that the displacement at the center of nanofilm must be bounded, the unknown arbitrary functions are obtained as

$$A_1 = -\frac{p_0\lambda_2(D^* I_1(\lambda_2) - D_2^* I_1(\lambda_2) - D^*\lambda_2 I_0(\lambda_2))}{\Delta} \tag{39a}$$

$$A_3 = -\frac{p_0\lambda_1(D^* J_1(\lambda_1) - D_2^* J_1(\lambda_1) - D^*\lambda_1 J_0(\lambda_1))}{\Delta} \tag{39b}$$

$$A_2 = A_4 = 0 \tag{39c}$$

in which

$$\Delta = kR(\lambda_1(D^* I_0(\lambda_2)J_1(\lambda_1) - D_2^* I_0(\lambda_2)J_1(\lambda_1) - D^*\lambda_1 I_0(\lambda_2)J_0(\lambda_1))$$

$$+\lambda_2(D^* I_1(\lambda_2)J_0(\lambda_1) - D_2^* I_1(\lambda_2)J_0(\lambda_1) - D^*\lambda_2 I_0(\lambda_2)J_0(\lambda_1))) \tag{40}$$

The boundary conditions for a circular nanofilm with clamped supported are

$$\frac{d\bar{w}(0)}{d\bar{r}} = \frac{d\bar{w}(1)}{d\bar{r}} = \bar{w}(1) = 0 \tag{41}$$

The following solutions for the unknown arbitrary functions can be obtained as

$$A_1 = -\frac{p_0\lambda_2 I_1(\lambda_2)}{kR\left[J_0(\lambda_1)\lambda_2 I_1(\lambda_2) + \lambda_1 I_0(\lambda_2)J_1(\lambda_1)\right]} \tag{42a}$$

$$A_3 = -\frac{p_0\lambda_1 J_1(\lambda_1)}{kR\left[J_0(\lambda_1)\lambda_2 I_1(\lambda_2) + \lambda_1 I_0(\lambda_2)J_1(\lambda_1)\right]}. \tag{42b}$$

$$A_2 = A_4 = 0 \tag{42c}$$

Response of Nanofilm on Winkler Support

The analytical solutions are implemented in a computer code to examine the fundamental responses of nanofilm-substrate systems. Nanofilms made of aluminium (Al) with elastic modulus E = 90 GPa and Poisson's ratio ν = 0.23 is

considered in the numerical analysis. In addition, the surface properties of aluminium are: λ^s = 3.4939 N/m, μ^s = -5.4251 N/m, and τ^s = 0.5689 N/m.

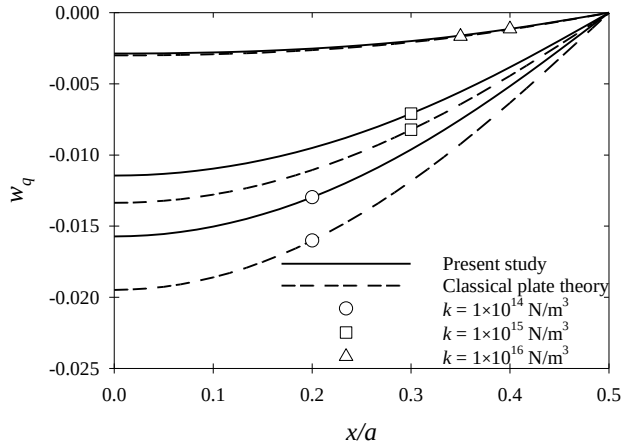

Figure 10 Normalized deflections of rectangular nanofilms on Winkler support (a = 200 nm, b = 200 nm, p_0 = 1 nN/nm).

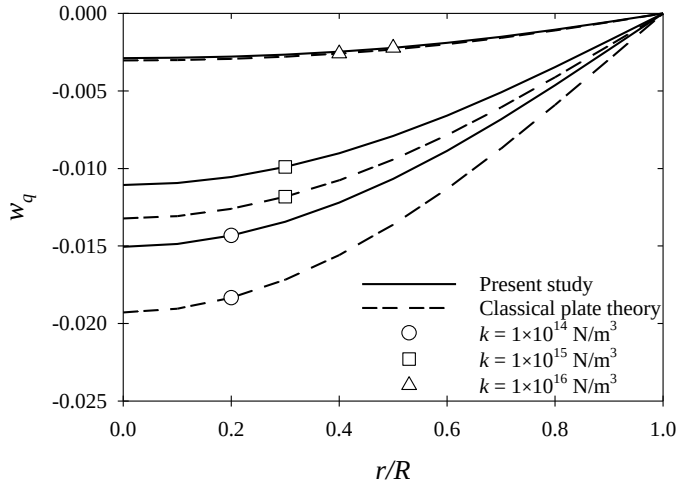

Figure 11 Normalized deflections of circular nanofilm on Winkler support (R = 100 nm, p_0 = 1 nN/nm).

The rectangular nanofilms with all edges simply-supported (SSSS) resting on a Winkler support and subjected to a uniformly distributed load p_0 is first examined. The case of nanofilm with dimensions a = 200 nm, b = 200 nm, t = 10 nm and applied loading p_0 = 1 nN/nm is considered in the numerical study. The normalized deflections of rectangular nanofilms, $w_0 = w/(p_0 a^2)$, are presented in Figure 10 for different values for stiffness of Winkler support, i.e., $k = 1\times10^{14}$,

1×10^{15} and 1×10^{16} N/m^3. The solutions for an identical classical plate theory (zero surface material parameters) are also presented in Figure 10, to investigate the influence of surface energy on nanofilm-substrate system. The classical solution is obtained from the present analysis by applying negligible values for surface material parameters. The normalized deflections, $w/(4p_0R^2)$, for a circular nanofilms (R = 100 nm) with simply supported edge resting on Winkler support and subjected to a uniformly distributed load (p_0 = 1 nN/nm) are also presented in Figure 11 for different values for stiffness of Winkler support. Based on the numerical results in Figures 10 and 11, the deflections of the nanofilm-substrate systems are decreased, as expected, by increasing the Winkler support stiffness, implying softer foundation, the solution become more applicable for larger k values. The influence of surface energy effects can also be observed from the numerical study shown in Figures 10 and 11. It can be seen from the numerical results that the deflections obtained from the analysis of nanofilm-substrate system with the consideration of surface energy effects are lower than its counterpart without the surface effects. This implies that surface energy effects incorporated in the nanofilms model make the nanofilms stiffer when the contribution of surface residual stress τ^s is positive. The term $-2\tau^s\nabla^2 w$ changes the structure of the governing equation from the classical plate theory case and make an influence on the response.

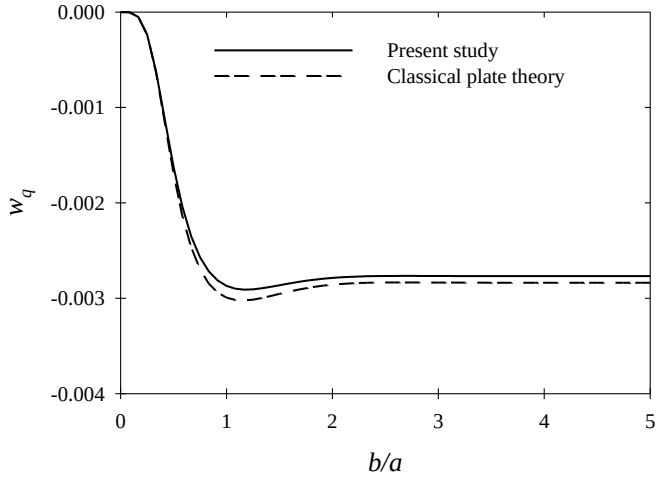

Figure 12 Normalized deflections of rectangular nanofilm with all edges simply supported (SSSS) on Winkler support with varying aspect ratio b/a (a = 200 nm, p_0 = 1 nN/nm, k = 1×1016 N/m^3).

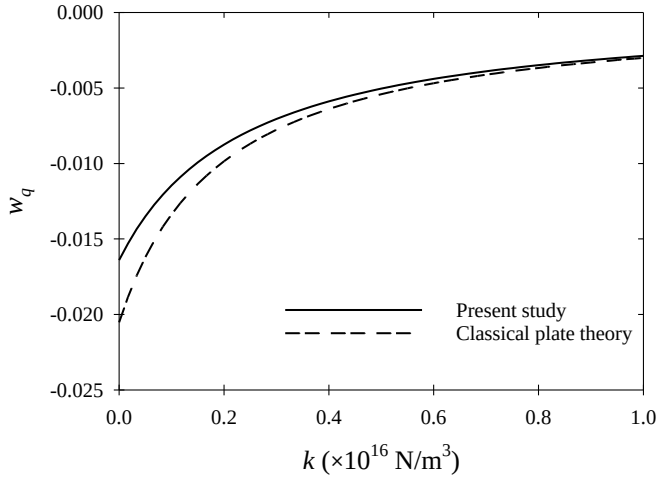

Figure 13 Normalized deflections of rectangular nanofilms on Winkler support with varying stiffness of Winkler support (a = 200 nm, b = 200 nm, p_0 = 1 nN/nm).

The central deflections of rectangular nanofilm with varying b dimension is presented in Figure 12 (a = 200 nm, p_0 = 1 nN/nm, k = 1×1016 N/m^3). The objective is to investigate the influence of nanofilm's aspect ratio b/a on the behavior of nanofilm-substrate system. It should be observed from the results in Figure 12 that the maximum central deflection occurs at the aspect ratio b/a close to 1.0. The deflection slightly decreases with increasing the aspect ratio b/a > 1.0 and eventually becomes almost constant when the aspect ratio b/a is greater than 3.0. This is because on increasing the aspect ratio the dimension of one of edges of the nanofilm increase which in turn increases the stiffness of the nanofilm therefore, decreasing the deflection.

Next, the influence of stiffness of Winkler support on nanofilm-substrate system is investigated. Figure 13 presents a central deflection profiles of rectangular nanofilm plotted with varying values of stiffness of Winkler support k in the range from zero up to 1×10^{16} N/m^3. These result clearly shows that the central deflections of nanofilm decrease with increasing of stiffness of Winkler support and theoretically converge to zero as the higher values of stiffness of Winkler support represents the more rigid the foundation for the nanofilm-substrate system. This implies that the Winkler support model is only a convenient approximation, the value of k depends on the load distribution and intensity as well as on the depth of the underlying material, but clearly emphasize the need for studying the nanofilm-substrate interaction to estimate the realistic behavior in the flexible foundation for the system.

4.3.2 Elastic Nanolayer on Winkler Support

Elastic nanolayer on Winkler support under vertical loadings are formulated for plane strain and axisymmetric cases as shown in Figure 14. A set of analytical techniques for stress and displacement fields corresponding to elastic nanolayer based on Love's representation, Hankel and Fourier integral transforms are adopted to derive an explicit integral form solutions for elastic nanolayer problems.

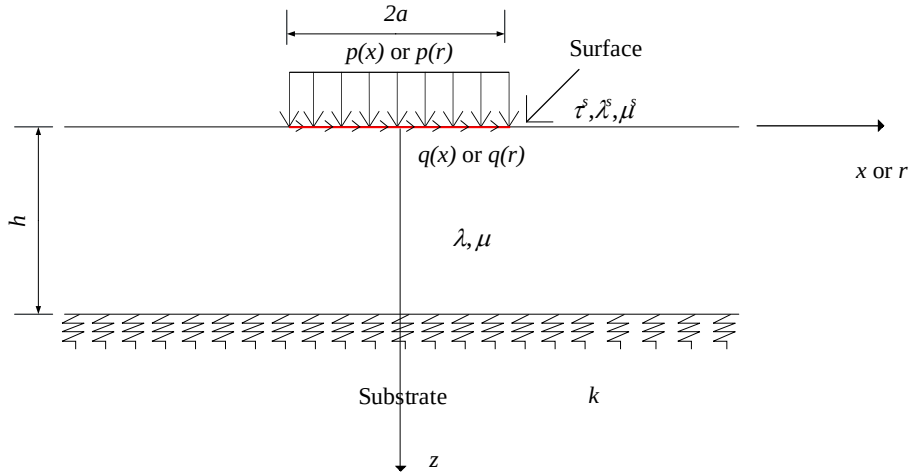

Figure 14 Nanolayer on Winkler support: plane strain and axisymmetric cases.

Plane Strain Case

In the absence of body forces, the three-dimensional equilibrium equation, constitutive equations and classical strain-displacement relationship of the bulk material are given respectively by,

$$\sigma_{ij,j} = 0 \tag{43a}$$

$$\sigma_{ij} = 2\mu\varepsilon_{ij} + \lambda\delta_{ij}\varepsilon_{kk} \tag{43b}$$

$$\varepsilon_{ij} = \frac{1}{2}(u_{i,j} + u_{j,i}) \tag{43c}$$

where σ_{ij}, ε_{ij} and u_i denote the components of stress, strain and displacement tensors, respectively; and are Lamé constants of the bulk material.

The equations of the bulk material in Eq. (43) of a two-dimensional elastic solid in the *x*-*z* plane, can be expressed as

$$\frac{\partial \sigma_{xx}}{\partial x} + \frac{\partial \sigma_{xz}}{\partial z} = 0 \tag{44a}$$

$$\frac{\partial \sigma_{zx}}{\partial x} + \frac{\partial \sigma_{zz}}{\partial z} = 0 \tag{44b}$$

$$\sigma_{xx} = (\lambda + 2\mu)\varepsilon_{xx} + \lambda \varepsilon_{zz} \tag{44c}$$

$$\sigma_{zz} = (\lambda + 2\mu)\varepsilon_{zz} + \lambda \varepsilon_{xx} \tag{44d}$$

$$\sigma_{xz} = \sigma_{zx} = 2\mu \varepsilon_{xz} \tag{44e}$$

$$\varepsilon_{xx} = \frac{\partial u_x}{\partial x} \tag{44f}$$

$$\varepsilon_{zz} = \frac{\partial u_z}{\partial z} \tag{44g}$$

$$\varepsilon_{xz} = \varepsilon_{zx} = \frac{1}{2}\left(\frac{\partial u_z}{\partial x} + \frac{\partial u_x}{\partial z} \right) \tag{44h}$$

Consider stress and traction components of an incremental element of the surface layer and bulk element as shown in Figure 15. The equation on the surface in Eqs. (1)-(3) can be written by

$$\frac{\partial \sigma_{xx}^s}{\partial x} + \sigma_{xz}\big|_{z=0} + T_x = 0 \tag{45a}$$

$$\frac{\partial \sigma_{zx}^s}{\partial x} + \sigma_{zz}\big|_{z=0} + T_z = 0 \tag{45b}$$

$$\sigma_{xx}^s = \tau^s + \kappa^s \varepsilon_{xx}^s \tag{45c}$$

$$\sigma_{zx}^s = \tau^s \frac{du_z^s}{dx} \tag{45d}$$

$$\varepsilon_{xx}^s = \frac{du_x^s}{dx} \tag{45e}$$

$$\frac{\partial \sigma_{xx}^s}{\partial x} + \sigma_{xz}\big|_{z=0} + T_x = 0 \tag{45f}$$

where $\kappa^s = \lambda^s + 2\mu^s$ is a surface material constant.

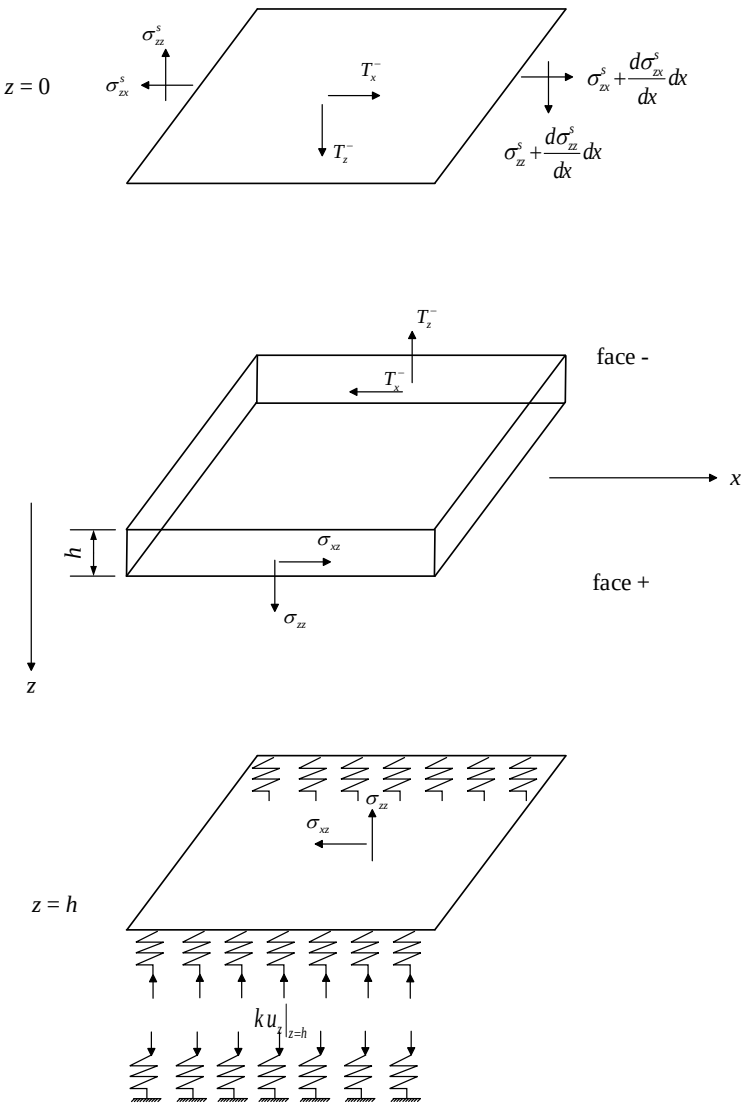

Figure 15 Stress and traction components of an incremental element of the surface layer and bulk element: plane strain case.

The general solution for the bulk material can be obtained by solving bi-harmonic equation,

$$\nabla_1^2 \nabla_1^2 \chi = 0 \tag{46}$$

where χ denotes Airy stress function.

By using Fourier integral transforms into Eq. (43) can be expressed as

$$\int_{-\infty}^{+\infty} \nabla_1^2 \nabla_1^2 \chi e^{i\xi x} dx = \left(\frac{d^2}{dz^2} - \xi^2 \right)^2 G(\xi, z) = 0 \tag{47}$$

where $G(\xi, z) = \int_{-\infty}^{+\infty} \chi e^{i\xi x} dx.$

The general solution of above equation may be written in the following form

$$G(\xi, z) = (A + Bz)e^{-|\xi|z} + (C + Dz)e^{|\xi|z} \tag{48}$$

where the arbitrary constants *A*, *B*, *C*, and *D* are calculated form the boundary conditions.

The general solutions for stresses and displacements of the bulk material by using Fourier integral transforms as

$$\sigma_{zz} = -\frac{1}{2\pi}\int_{-\infty}^{+\infty} \xi^2 G e^{-i\xi x} d\xi \tag{49a}$$

$$\sigma_{xx} = \frac{1}{2\pi}\int_{-\infty}^{+\infty} \frac{d^2 G}{dz^2} e^{-i\xi x} d\xi \tag{49b}$$

$$\sigma_{xz} = \frac{1}{2\pi}\int_{-\infty}^{+\infty} i\xi \frac{dG}{dz} e^{-i\xi x} d\xi \tag{49c}$$

$$u_z = \frac{1}{8\pi\mu(\lambda+\mu)}\int_{-\infty}^{+\infty} \left[(\lambda + 2\mu)\frac{d^3 G}{dz^3} - (3\lambda + 4\mu)\xi^2 \frac{dG}{dz} \right] e^{-i\xi x} \frac{d\xi}{\xi^2} \tag{49d}$$

$$u_x = \frac{1}{8\pi\mu(\lambda+\mu)}\int_{-\infty}^{+\infty} \left[(\lambda + 2\mu)\frac{d^2 G}{dz^2} + \lambda\xi^2 G \right] i e^{-i\xi x} \frac{d\xi}{\xi} \tag{49e}$$

The boundary conditions are given by

$$\sigma_{zz}^s\Big|_{z=0} + \left(\frac{d\tau^s}{dx}\frac{du_z^s}{dx}\Big|_{z=0} + \tau^s \frac{d^2 u_z^s}{dx^2}\Big|_{z=0} \right) = -p(x) \tag{50a}$$

$$\sigma_{zx}^s\Big|_{z=0} + \left(\frac{d\tau^s}{dx} + \kappa^s \frac{d^2 u_x^s}{dx^2}\Big|_{z=0} \right) = -q(x) \tag{50b}$$

$$\sigma_{zz}\Big|_{z=h} = -k\, u_z\Big|_{z=h} \tag{50c}$$

$$\sigma_{zx}\Big|_{z=h} = 0 \tag{50d}$$

The arbitrary functions can be constituted by applying Fourier integral transforms to Eqs. (50a) to (50d) together with the assumption that the residual

surface stress is constant.

$$A\left(1+\frac{\tau^s|\xi|}{2\mu}\right)+B\left(\frac{\tau^s}{2(\lambda+u)}\right)+C\left(1-\frac{\tau^s|\xi|}{2\mu}\right)+D\left(\frac{\tau^s}{2(\lambda+u)}\right)=\frac{\bar{p}(\xi)}{\xi^2} \tag{51a}$$

$$A|\xi|\left(1+\frac{\Lambda|\xi|(\lambda+u)}{(\lambda+2\mu)}\right)-B\left(1+\Lambda|\xi|\right)-C|\xi|\left(1-\frac{\Lambda|\xi|(\lambda+u)}{(\lambda+2\mu)}\right)-D\left(1-\Lambda|\xi|\right)$$
$$=\frac{\bar{q}(\xi)}{i\xi} \tag{51b}$$

$$A\left(1-\frac{k}{2\mu|\xi|}\right)e^{-|\xi|h}+B\left[h-\frac{k}{2|\xi|}\left(\frac{h}{\mu}+\frac{1}{|\xi|(\lambda+u)}\right)\right]e^{-|\xi|h}+C\left(1+\frac{k}{2\mu|\xi|}\right)e^{|\xi|h}$$
$$+D\left[h+\frac{k}{2|\xi|}\left(\frac{h}{\mu}-\frac{1}{|\xi|(\lambda+u)}\right)\right]e^{|\xi|h}=0 \tag{51c}$$

$$A|\xi|e^{-|\xi|h}-B\left(1-h|\xi|\right)e^{-|\xi|h}-C\left(|\xi|\right)e^{|\xi|h}-D\left(1+h|\xi|\right)e^{|\xi|h}=0 \tag{51d}$$

where $\bar{p}(\xi)$ and $\bar{q}(\xi)$ are the Fourier transforms of vertical and horizontal loading, respectively.

The following solutions for the unknown arbitrary functions can be obtained:

$$\bar{p}(\xi)=\int_{-\infty}^{+\infty}p(x)e^{-i\xi x}dx \tag{52a}$$

$$\bar{q}(\xi)=\int_{-\infty}^{+\infty}q(x)e^{-i\xi x}dx \tag{52b}$$

For the cases of uniformly distributed vertical load of constant magnitude p_0

$$\bar{p}(\xi)=\frac{2\sin(\xi a)}{\xi}p_0 \tag{53}$$

Note that $\Lambda=\frac{\kappa^s(\lambda+2\mu)}{2\mu(\lambda+\mu)}$ is a parameter with a dimension of length and represents a ratio of surface to bulk elastic properties. This parameter can be viewed as material characteristic length that represents the influence of surface stress.

$$[K][X] = [F] \tag{54a}$$

or

$$\begin{bmatrix} 1+\dfrac{\tau^s|\xi|}{2\mu} & \dfrac{\tau^s}{2(\lambda+u)} & 1-\dfrac{\tau^s|\xi|}{2\mu} & \dfrac{\tau^s}{2(\lambda+u)} \\ |\xi|\left(1+\dfrac{\Lambda|\xi|(\lambda+u)}{(\lambda+2\mu)}\right) & -\left(1+\Lambda|\xi|\right) & -|\xi|\left(1-\dfrac{\Lambda|\xi|(\lambda+u)}{(\lambda+2\mu)}\right) & -\left(1-\Lambda|\xi|\right) \\ \left(1-\dfrac{k}{2\mu|\xi|}\right)e^{-|\xi|h} & \left[h-\dfrac{k}{2|\xi|}\left(\dfrac{h}{\mu}+\dfrac{1}{|\xi|(\lambda+u)}\right)\right]e^{-|\xi|h} & \left(1+\dfrac{k}{2\mu|\xi|}\right)e^{|\xi|h} & \left[h+\dfrac{k}{2|\xi|}\left(\dfrac{h}{\mu}-\dfrac{1}{|\xi|(\lambda+u)}\right)\right]e^{|\xi|h} \\ |\xi|e^{-|\xi|h} & -\left(1-h|\xi|\right)e^{-|\xi|h} & -|\xi|e^{|\xi|h} & -\left(1+h|\xi|\right)e^{|\xi|h} \end{bmatrix} \begin{Bmatrix} A \\ B \\ C \\ D \end{Bmatrix} = \begin{Bmatrix} \dfrac{\bar{p}(\xi)}{\xi^2} \\ \dfrac{\bar{q}(\xi)}{i|\xi|} \\ 0 \\ 0 \end{Bmatrix} \tag{54b}$$

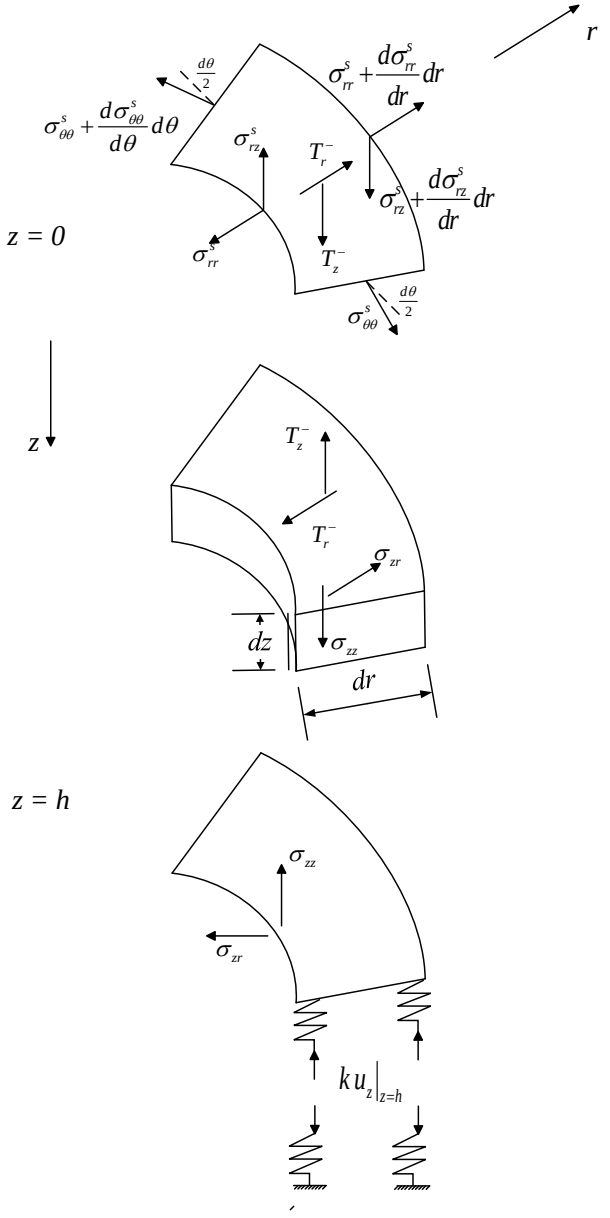

Figure 16 Stress and traction components of an incremental element of the surface layer and bulk element: axisymmetric case.

Axisymmetric Case

Consider stress and traction components of an incremental element of the surface layer and bulk element as shown in Figure 16. The equations of the bulk material in the *r*-*z* plane can be expressed as

$$\frac{\partial \sigma_{rr}}{\partial r} + \frac{\partial \sigma_{rz}}{\partial z} + \frac{\sigma_{rr} - \sigma_{\theta\theta}}{r} = 0 \tag{55a}$$

$$\frac{\partial \sigma_{rz}}{\partial r} + \frac{\partial \sigma_{zz}}{\partial z} + \frac{\sigma_{rz}}{r} = 0 \tag{55b}$$

$$\sigma_{rr} = (\lambda + 2\mu)\varepsilon_{rr} + \lambda\varepsilon_{\theta\theta} + \lambda\varepsilon_{zz} \tag{55c}$$

$$\sigma_{\theta\theta} = \lambda\varepsilon_{rr} + (\lambda + 2\mu)\varepsilon_{\theta\theta} + \lambda\varepsilon_{zz} \tag{55d}$$

$$\sigma_{zz} = \lambda\varepsilon_{rr} + \lambda\varepsilon_{\theta\theta} + (\lambda + 2\mu)\varepsilon_{zz} \tag{55e}$$

$$\sigma_{rz} = \sigma_{zr} = 2\mu\varepsilon_{rz} \tag{55f}$$

$$\varepsilon_{rr} = \frac{\partial u_r}{\partial r} \tag{55g}$$

$$\varepsilon_{\theta\theta} = \frac{u_r}{r} \tag{55h}$$

$$\varepsilon_{zz} = \frac{\partial u_z}{\partial z} \tag{55i}$$

$$\varepsilon_{rz} = \varepsilon_{zr} = \frac{1}{2}\left(\frac{\partial u_r}{\partial z} + \frac{\partial u_z}{\partial r} \right) \tag{55j}$$

The equations on the surface in Eqs. (1)-(3) are given by

$$\frac{d\sigma_{rr}^s}{dr} + \frac{\sigma_{rr}^s - \sigma_{\theta\theta}^s}{r} + \sigma_{zr}\big|_{z=0} + T_r = 0 \tag{56a}$$

$$\frac{d\sigma_{zr}^s}{dr} + \frac{\sigma_{zr}^s}{r} + \sigma_{zz}\big|_{z=0} + T_z = 0 \tag{56b}$$

$$\sigma_{rr}^s = \tau^s + (\lambda^s + 2\mu^s)\varepsilon_{rr}^s + (\lambda^s + \tau^s)\varepsilon_{\theta\theta}^s \tag{56c}$$

$$\sigma_{\theta\theta}^{s} = \tau^{s} + (\lambda^{s} + 2\mu^{s})\varepsilon_{\theta\theta}^{s} + (\lambda^{s} + \tau^{s})\varepsilon_{rr}^{s} \tag{56d}$$

$$\sigma_{zr}^{s} = \tau^{s} \frac{du_{z}^{s}}{dr} \tag{56e}$$

$$\varepsilon_{rr}^{s} = \frac{du_{r}^{s}}{dr} \tag{56f}$$

$$\varepsilon_{\theta\theta}^{s} = \frac{u_{r}^{s}}{r} \tag{56f}$$

The general solution for the bulk material can be obtained by solving bi-harmonic equation,

$$\nabla_{2}^{2}\nabla_{2}^{2}\phi = 0 \tag{57}$$

where ϕ denotes Love's strain potential.

Applying Hankel integral transform to the bi-harmonic equation Eq. (57) leads to,

$$\int_{0}^{\infty} \nabla_{2}^{2}\nabla_{2}^{2}\phi J_{0}(\xi r) r dr = \left(\frac{d^{2}}{dz^{2}} - \xi^{2} \right)^{2} \Omega(\xi, z) = 0 \tag{58}$$

where $\Omega(\xi, z) = \int_{0}^{\infty} r\phi J_{0}(\xi r) dr$ and $J_{n}(\xi)$ denotes the Bessel functions of the first kind of order *n*.

The general solution of homogeneous ordinary differential equation is given by

$$\Omega(\xi, z) = (E + Fz)e^{-|\xi|z} + (G + Hz)e^{|\xi|z} \tag{59}$$

where the arbitrary constants *E*, *F*, *G* and *H* are calculated form the boundary conditions.

The general solutions for stresses and displacements of the bulk material in Hankel integral transforms are

$$\sigma_{rr} = \int_{0}^{\infty} \xi \left[\lambda \frac{d^{3}\Omega}{dz^{3}} + (\lambda + 2\mu)\xi^{2} \frac{d\Omega}{dz} \right] J_{0}(\xi r) d\xi - \frac{2(\lambda + \mu)}{r} \int_{0}^{\infty} \frac{d\Omega}{dz} J_{1}(\xi r) d\xi \tag{60a}$$

$$\sigma_{\theta\theta} = \lambda\int_0^\infty \xi\left[\frac{d^3\Omega}{dz^3} - \xi^2\frac{d\Omega}{dz}\right]J_0(\xi r)d\xi + \frac{2(\lambda+\mu)}{r}\int_0^\infty \xi^2\frac{d\Omega}{dz}J_1(\xi r)d\xi \tag{60b}$$

$$\sigma_{zz} = \int_0^\infty \xi\left[(\lambda+2\mu)\frac{d^3\Omega}{dz^3} - (3\lambda+4\mu)\xi^2\frac{d\Omega}{dz}\right]J_0(\xi r)d\xi \tag{60c}$$

$$\sigma_{rz} = \int_0^\infty \xi^2\left[\lambda\frac{d^2\Omega}{dz^2} + (\lambda+2\mu)\xi^2\Omega\right]J_1(\xi r)d\xi \tag{60d}$$

$$u_r = \frac{\lambda+\mu}{\mu}\int_0^\infty \xi^2\frac{d\Omega}{dz}J_1(\xi r)d\xi \tag{60e}$$

$$u_z = \int_0^\infty \xi\left[\frac{d^2\Omega}{dz^2} - \frac{(\lambda+2\mu)}{\mu}\xi^2\Omega\right]J_0(\xi r)d\xi \tag{60f}$$

The boundary conditions can be written as

$$\sigma_{zz}^s\Big|_{z=0} + \left[\frac{d\tau^s}{dr}\frac{du_z^s}{dr}\Big|_{z=0} + \tau^s\left(\frac{d^2u_z^s}{dr^2} + \frac{1}{r}\frac{du_z^s}{dr}\right)_{z=0}\right] = -p(r) \tag{61a}$$

$$\sigma_{zr}^s\Big|_{z=0} + \left[\frac{d\tau^s}{dr}\left(1+\frac{u_r^s}{r}\right)\Big|_{z=0} + \kappa^s\left(\frac{d^2u_r^s}{dr^2} + \frac{1}{r}\frac{du_r^s}{dr} - \frac{u_r^s}{r^2}\right)\Big|_{z=0}\right] = -q(r) \tag{61b}$$

$$\sigma_{zz}\Big|_{z=h} = -k\,u_z\Big|_{z=h} \tag{61c}$$

$$\sigma_{zr}\Big|_{z=h} = 0 \tag{61d}$$

The arbitrary functions can be constituted by applying Hankel integral transforms to Eqs. (61a)-(61d) can be expressed as

$$E\left(1+\frac{\tau^s|\xi|}{2\mu}\right)|\xi|(\lambda+\mu) + F\left(\mu+\tau^s|\xi|\right) - G\left(1-\frac{\tau^s|\xi|}{2\mu}\right)|\xi|(\lambda+\mu) + H\left(\mu-\tau^s|\xi|\right) = -\frac{\overline{p}'(\xi)}{2\xi^2} \tag{62a}$$

$$E\left(1+\frac{\Lambda|\xi|(\lambda+\mu)}{(\lambda+2\mu)}\right)|\xi|(\lambda+\mu) - F\left(\lambda+\frac{\Lambda|\xi|(\lambda+u)^2}{(\lambda+2\mu)}\right) + G\left(1-\frac{\Lambda|\xi|(\lambda+\mu)}{(\lambda+2\mu)}\right)|\xi|(\lambda+\mu) + H\left(\lambda-\frac{\Lambda|\xi|(\lambda+u)^2}{(\lambda+2\mu)}\right) = -\frac{\overline{q}'(\xi)}{2\xi^2} \tag{62b}$$

$$E\left(1-\frac{k}{2\mu|\xi|}\right)|\xi|(\lambda+\mu)e^{-|\xi|h}+F\left(\frac{\mu}{\lambda+\mu}+h|\xi|-k\left[\frac{h}{2\mu}+\frac{1}{|\xi|(\lambda+\mu)}\right]\right)(\lambda+\mu)e^{-|\xi|h}$$

$$-G\left(1+\frac{k}{2\mu|\xi|}\right)|\xi|(\lambda+\mu)e^{|\xi|h}+H\left(\frac{\mu}{\lambda+\mu}-h|\xi|+k\left[\frac{1}{|\xi|(\lambda+\mu)}-\frac{h}{2\mu}\right]\right)(\lambda+\mu)e^{|\xi|h}=0 \tag{62c}$$

$$E\left(|\xi|(\lambda+\mu)\right)e^{-|\xi|h}+F\left(h|\xi|(\lambda+\mu)-\lambda\right)e^{-|\xi|h}+G\left(|\xi|(\lambda+\mu)\right)e^{|\xi|h}$$
$$+H\left(h|\xi|(\lambda+\mu)+\lambda\right)e^{|\xi|h}=0 \tag{62d}$$

where $\bar{p}'(\xi)$ and $\bar{q}'(\xi)$ are the Hankel transforms of normal and tangential loading, respectively.

$$\bar{p}'(\xi)=-\int_0^\infty rp(r)J_0(\xi r)dr \tag{63a}$$

$$\bar{q}'(\xi)=-\int_0^\infty rq(r)J_1(\xi r)dr \tag{63b}$$

For the cases of uniformly distributed vertical load of constant magnitude p_0

$$\bar{p}'(\xi)=\frac{aJ_1(\xi a)}{\xi}p_0 \tag{64}$$

$$[K']\{X'\}=\{F'\} \tag{65a}$$

where

$$[K]=\begin{bmatrix} |\xi|(\lambda+\mu)\left(1+\frac{\tau^s|\xi|}{2\mu}\right) & \mu+\tau^s|\xi| & -|\xi|(\lambda+\mu)\left(1-\frac{\tau^s|\xi|}{2\mu}\right) & \mu-\tau^s|\xi| \\ |\xi|(\lambda+\mu)\left(1+\frac{\Lambda|\xi|(\lambda+\mu)}{(\lambda+2\mu)}\right) & -\left(\lambda+\frac{\Lambda|\xi|(\lambda+u)^2}{(\lambda+2\mu)}\right) & |\xi|(\lambda+\mu)\left(1-\frac{\Lambda|\xi|(\lambda+\mu)}{(\lambda+2\mu)}\right) & \left(\lambda-\frac{\Lambda|\xi|(\lambda+u)^2}{(\lambda+2\mu)}\right) \\ |\xi|(\lambda+\mu)\left(1-\frac{k}{2\mu|\xi|}\right)e^{-|\xi|h} & (\lambda+\mu)\left(\frac{\mu}{\lambda+\mu}+h|\xi|-k\left[\frac{h}{2\mu}+\frac{1}{|\xi|(\lambda+\mu)}\right]\right)e^{-|\xi|h} & -|\xi|(\lambda+\mu)\left(1+\frac{k}{2\mu|\xi|}\right)e^{|\xi|h} & (\lambda+\mu)\left(\frac{\mu}{\lambda+\mu}-h|\xi|+k\left[\frac{1}{|\xi|(\lambda+\mu)}-\frac{h}{2\mu}\right]\right)e^{|\xi|h} \\ |\xi|(\lambda+\mu)e^{-|\xi|h} & \left(h|\xi|(\lambda+\mu)-\lambda\right)e^{-|\xi|h} & |\xi|(\lambda+\mu)e^{|\xi|h} & \left(h|\xi|(\lambda+\mu)+\lambda\right)e^{|\xi|h} \end{bmatrix}$$

$$\{X'\}=\begin{Bmatrix} E \\ F \\ G \\ H \end{Bmatrix}\{F'\}=\begin{Bmatrix} -\frac{\bar{p}'(\xi)}{2\xi^2} \\ -\frac{\bar{q}'(\xi)}{2\xi^2} \\ 0 \\ 0 \end{Bmatrix}, \tag{65b}$$

Accuracy of the present solutions for elastic nanolayer on Winkler support is first verified with two available benchmark solutions. The results obtained from the present formulation are first compared with the solutions reported by Intarit et al. (2011) for the case of a rigid-based elastic nanolayer under uniformly vertical load. Without the implemeatation of surface stresses into the model, the present numerical results are verified with the classical solutions of an elastic layer on Winkler support under line load and uniformly distributed vertical load presented by Dempsey (1990).

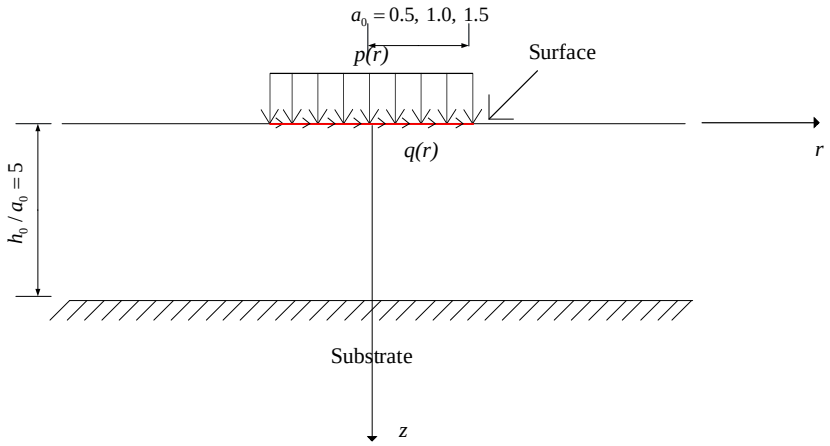

Figure 17 Elastic nanolayer resting on a rigid substrate (axisymmetric case) considered by Intarit et al. (2011).

Intarit et al. (2011) considered the case of elastic nanolayer resting on a rigid substrate as shown in Figure 17. A surface load is applied to the surface of a nanolayer over a circular area of normalized region $a_0 = a / \Lambda$. The material properties of the nanolayer considered by Intarit et al. (2011) are: λ = 58.17×109 N/m^2, μ = 26.13×109 N/m^2 and the surface properties are λ^s = 6.8511 N/m, μ^s = -0.376 N/m, τ^s = 5 N/m and material characteristic length is Λ = 1 nm. Different values of a_0. i.e., a_0 = 0.5, 1.0, and 1.5 are considered by Intarit et al. (2011) with normalized layer thickness h_0 / a_0 = 5. For a comparison purpose, the same set of material constants considered by Intarit et al. (2011) is utilized in the present numerical analysis. Numerical results for the case of a nanolayer with rigid-base can be obtained by the present formulation by setting displacement at $z = h$ is equal to zero and inputting large value of k.

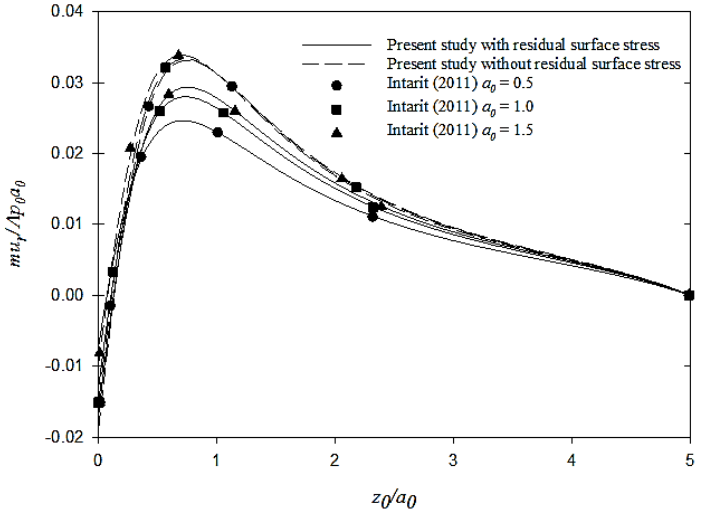

(a) Radial displacement

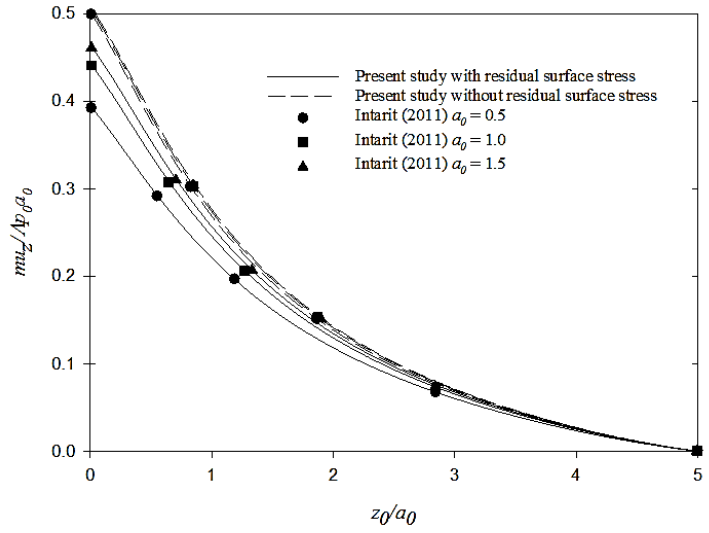

(b) Vertical displacement

Figure 18 Comparison of (a) radial displacement and (b) vertical displacement along *z*-axis due to uniformly distributed normal traction in an axisymmetric, rigid-based elastic nanolayer (Intarit et al., 2011).

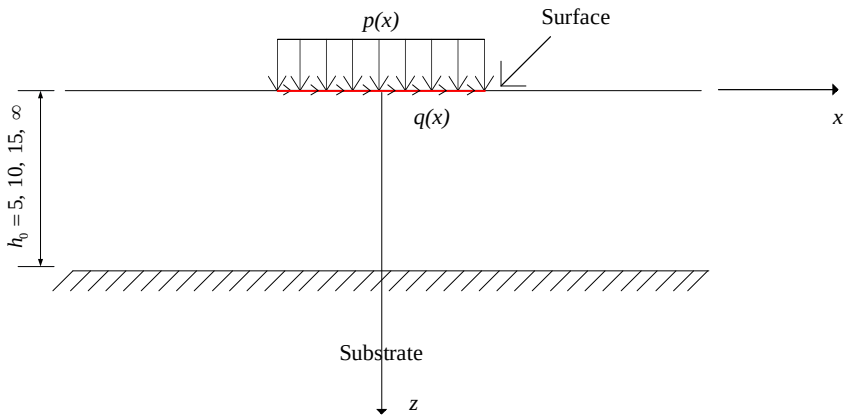

Figure 19 Elastic nanolayer resting on a rigid substrate (plane strain case) considered by Intarit et al. (2011).

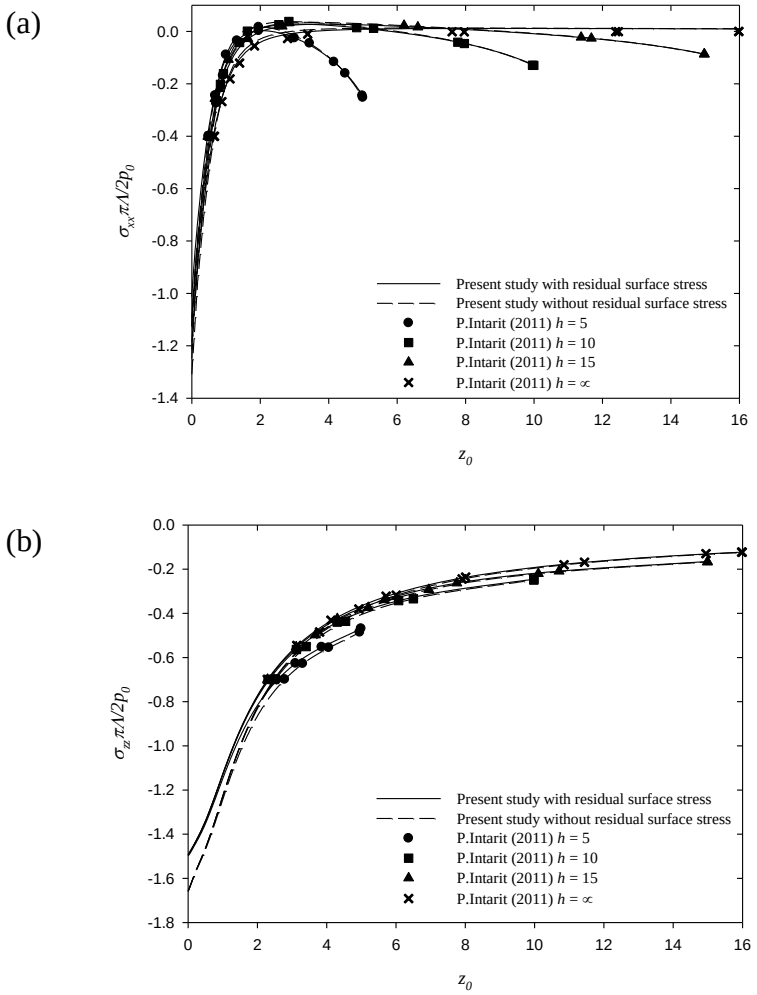

Figure 20 Comparison of stresses along z-axis due to uniformly distributed normal traction in a plane strain, rigid-based elastic nanolayer (Intarit et al., 2011)

The comparison of the present numerical results for radial and vertical displacements with Intarit et al. (2011) are illustrated in Figures 18(a) and (b) respectively. It can be seen from Figures 18(a) and (b) that the present numerical results are in excellent agreement with those given by Intarit et al. (2011) for both radial and vertical displacements. Additional comparison for a plane strain case (Figure 19) with different values of layer thicknesses h_0 = 5, 10, 15, and ∞ is shown in Figure 20. The numerical results obtained from the present study are again in excellent agreement with those given by Intarit et al. (2011) confirming the validation and accuracy of the present formulation scheme for both axisymmetric and plane strain cases of nanolayers on rigid substrates.

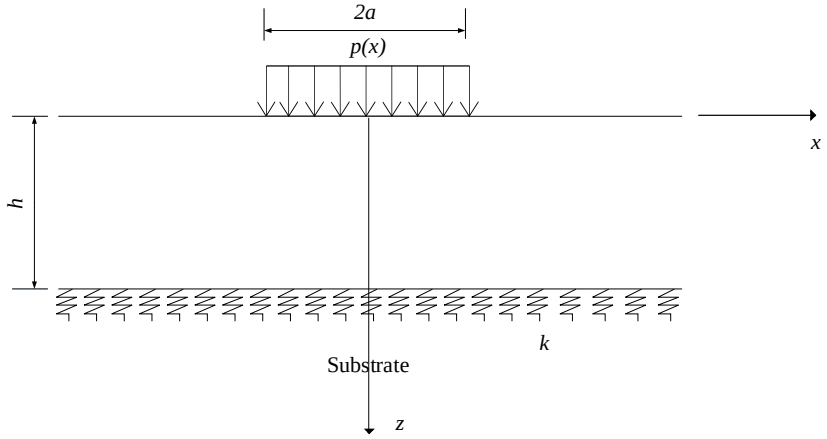

Figure 21 Comparison of surface deflection under uniformly distributed vertical load (Dempsey et al., 1990).

Figure 22 shows a comparison with the results presented by Dempsey et al. (1990) for the case of an elastic layer (without surface energy effects) resting on Winkler support subjected to a uniformly distributed vertical load. The schematic model is shown in Figure 21. Moreover, an elastic layer (without surface energy effects) resting on Winkler support subjected to a vertical line load is schematically presented in Figure 23 and the comparison for this case is presented in Figure 24. Material constants considered by Dempsey et al. (1990) are: ν = 0.25 and E = 1 N/m^2 with varying l/h values, where l/h = (E/12hk)$^{1/4}$. Results for this case can be obtained from the present formulation by setting $\tau^s = 0$ and $\Lambda = 0$ respectively. It can be seen from Figures 22 and 24 that the solutions of deflections obtained from the present model agree closely at all points with those given by Dempsey et al. (1990).

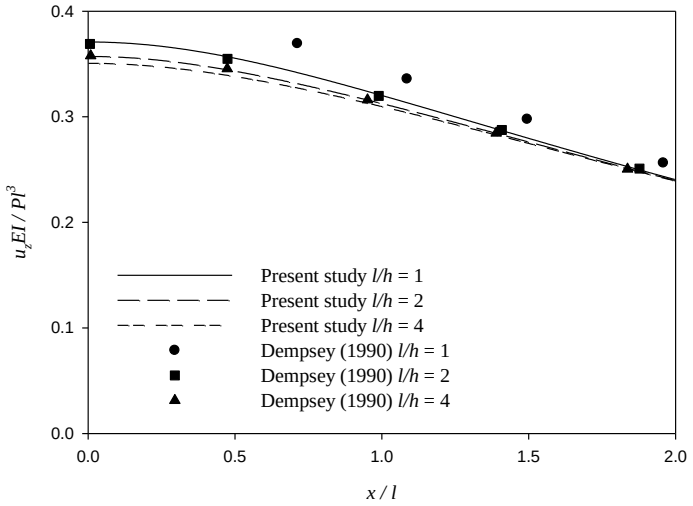

(a) Lower surface

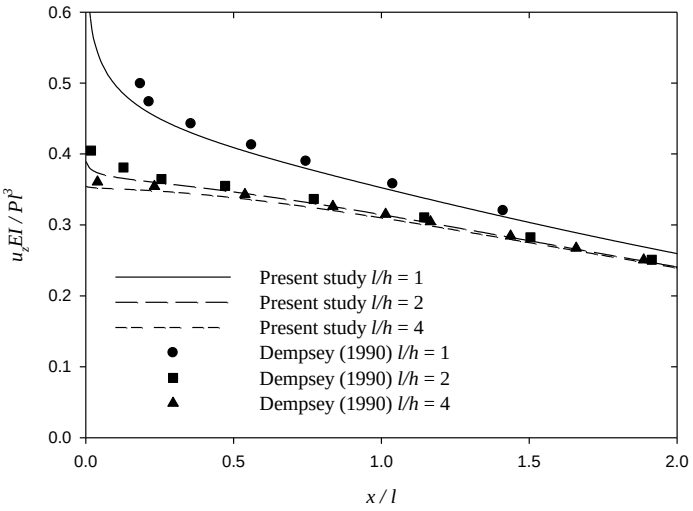

(b) Upper surface

Figure 22 Comparison of vertical deflections under uniformly distributed vertical load (Dempsey et al., 1990).

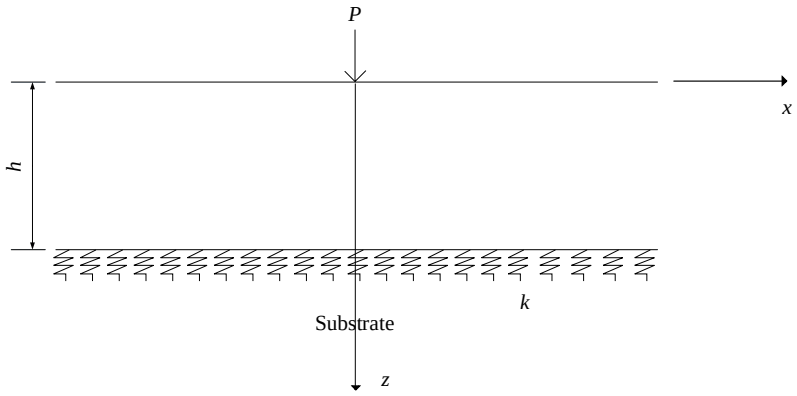

Figure 23 Comparison of surface deflection under line load (Dempsey et al., 1990).

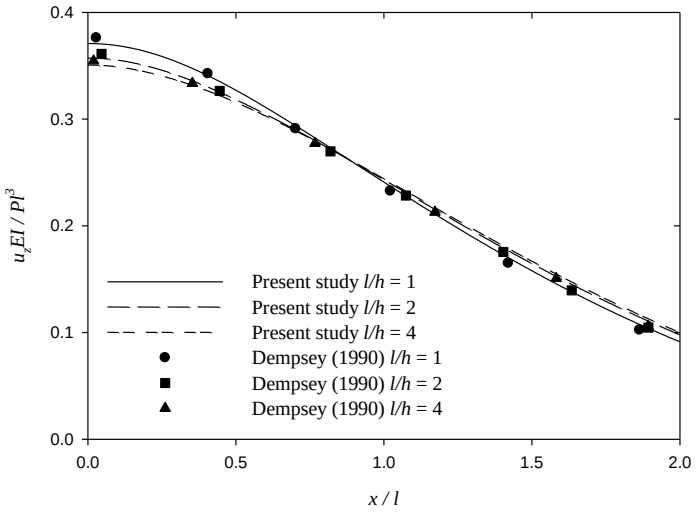

(a) Lower surface

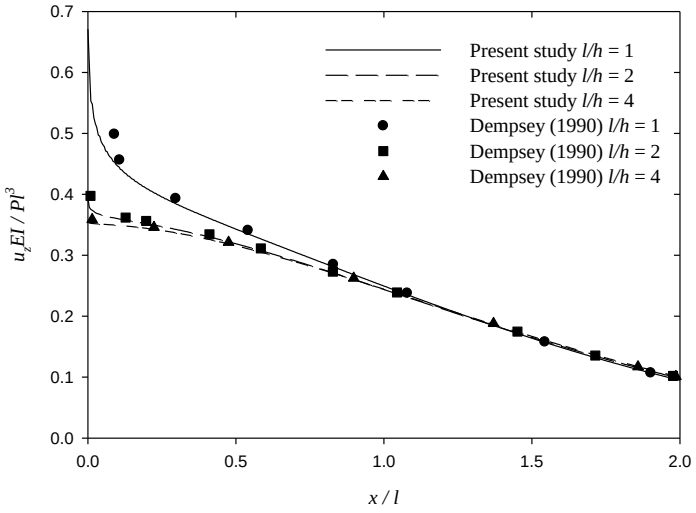

(b) Upper surface

Figure 24 Comparison of vertical displacement under line load (Dempsey et al., 1990).

Next, numerical results on stresses and displacements are presented to demonstrate the size-dependent behavior of an elastic nanolayer on Winkler support under vertical loadings. The explicit integral form solutions for plane strain and axisymmetric cases are evaluated by using globally adaptive numerical quadrature scheme based on 21-point Gauss-Kronrod rule. The properties of material considered in the numerical study are: λ = 58.17×109 N/m2, μ = 26.13×109 N/m2 for bulk material and λ^s = 6.8511 N/m, μ^s = -0.376 N/m, τ^s = 0.5689 N/m for surface material (Shenoy, 2000; Miller and Shenoy, 2000). Note that this set of material properties is employed for the rest of the numerical study presented hereafter. Non-dimensional variables are introduced in the present analysis, i.e., a non-dimensional elastic layer thickness $h_0 = h/\Lambda$; non-dimensional coordinates $x_0 = x/\Lambda$ and $z_0 = z/\Lambda$ for plane strain case and $r_0 = r/\Lambda$ for axisymmetric case.

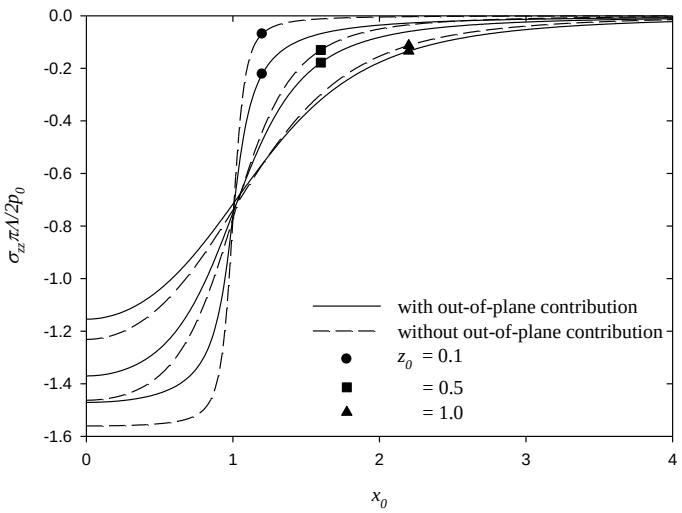

(a) σ_{zz}

Figure 25 Variation of stresses along the *x*-axis for a rigid-based elastic nanolayer with layer thickness (h_0 = 10) for various depth z_0 .

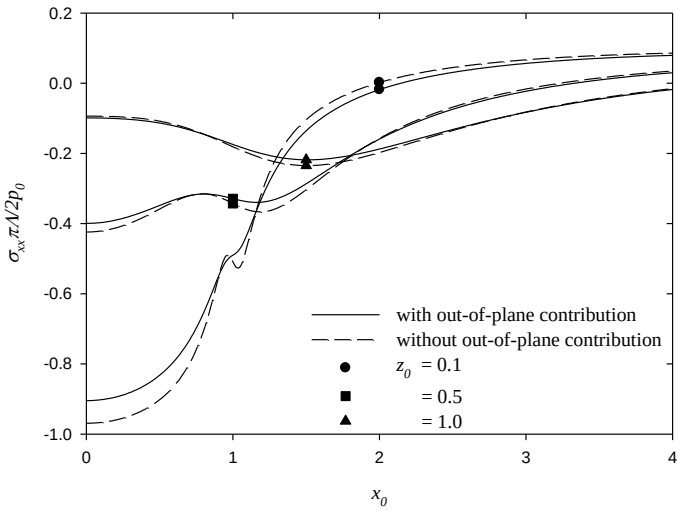

(b) σ_{xx}

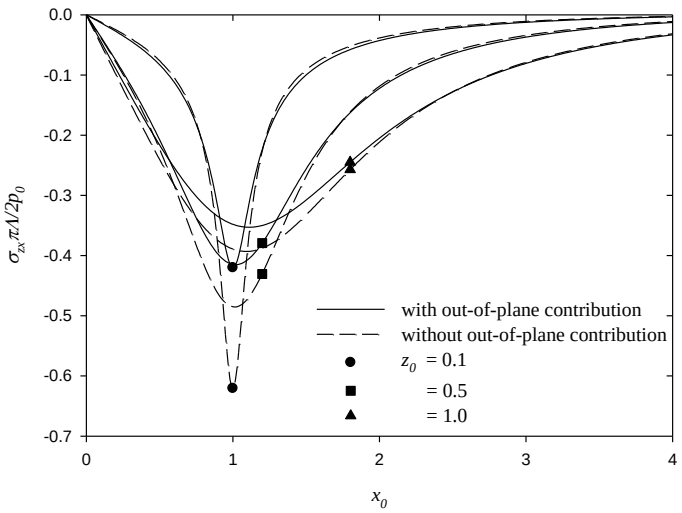

(c) σ_{zx}

Figure 25 Variation of stresses along the x-axis for a rigid-based elastic nanolayer with layer thickness ($h_0 = 10$) for various depth z_0 (Continue).

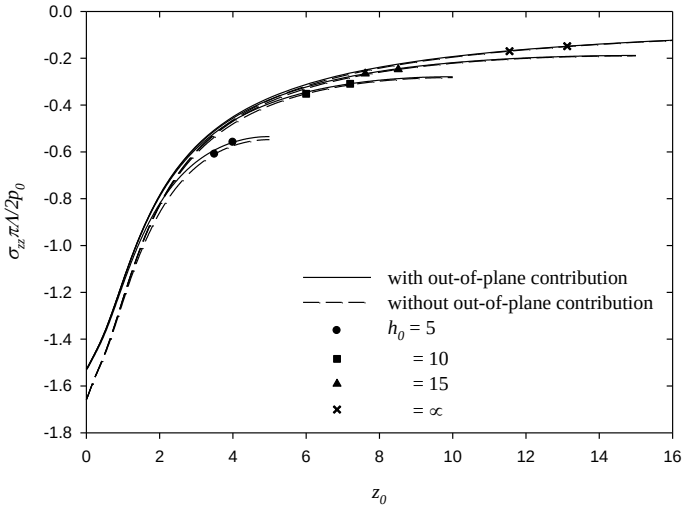

(a) σ_{zz}

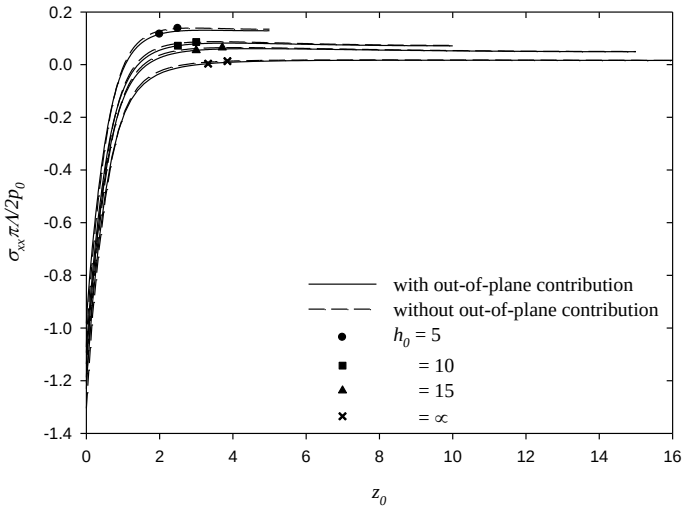

(b) σ_{xx}

Figure 26 Variation of stresses along the *z*-axis for a rigid-based elastic nanolayer with different layer thicknesses.

Figure 25 shows the distribution of vertical and horizontal stresses along the *x*-direction at different depths of a nanolayer with layer thickness h_0 = 10 under uniformly distributed vertical load over a region with a_0 = 1 at the surface. Only the solutions along the positive x-axis are plotted due to the symmetry or anti-symmetry of the solutions. The solid and dashed lines denote the solutions with and without out-of-plane contribution respectively. The stresses are mainly compressive and decrease with increasing depth from the free surface. It is evident from the results in Figure 25 that the consideration of the out-of-plane term in the analysis has a significant influence on the distribution of stress fields in a nanolayer. The out-of-plane contribution mostly influence vertical and shear stresses whereas horizontal stress shows a relatively negligible influence except near the loading area ($x_0 < 1$). This implies that the out-of-plane contribution is generally cannot be neglected in the analysis of a nanolayer.

The influence of the layer thickness on the non-dimensional stresses of a finite elastic nanolayer with thickness h_0 resting on a rigid base substrate is presented in Figure 26. The rigid-based elastic layer subjected to uniformly distributed vertical load over a region with a_0 = 1 at the free surface. The numerical results in Figure 26 are presented for different values of the nanolayer thicknesses, i.e., h_0 = 5, 10, 15, and ∞; and for both with and without out-of-plane contribution. The numerical results in Figure 26 reveal that the stress fields are significantly influenced by the thickness of a nanolayer. In particular, the vertical and horizontal stresses decrease with increasing elastic layer thickness. The influence of surface elasticity on finite elastic nanolayer resting on a rigid base substrate has been investigated by Zhao and Rajapakse (2009). However, the out-of-plane contribution from the residual surface tension is not considered in the study by Zhao and Rajapakse (2009).

The influence of stiffness of supporting material on the behavior of an elastic nanolayer is presented in Figure 27. An elastic nanolayer with h_0 = 10 subjected to a uniformly distributed vertical load over a region with a_0 = 1 at the free surface and supported by the Winkler-type foundation is considered in the numerical study. Different values of the support stiffness are considered, i.e., k/μ = 0.1, 1, and 10. It is noted that higher value of k/μ represents a stiffer supporting material. It can be seen in Figure 27 that stress fields in the nanolayer from both with and without out-of-plane contribution analysis are influenced by the stiffness of supporting material. The vertical stresses increase in the nanolayer resting on a

stiff material, e.g., k/μ=10. The distribution of horizontal stresses are more complicated than those of vertical stresses. It should be observed that higher tensile horizontal stress is generated for the case of a nanolayer resting on a soft supporting material.

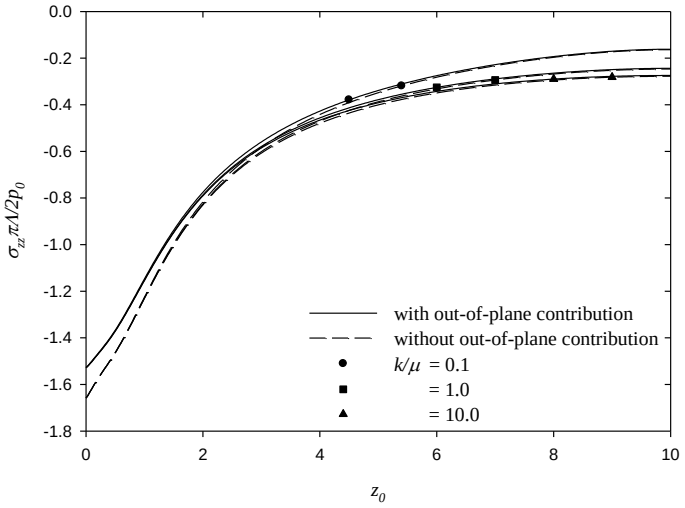

(a) σ_{zz}

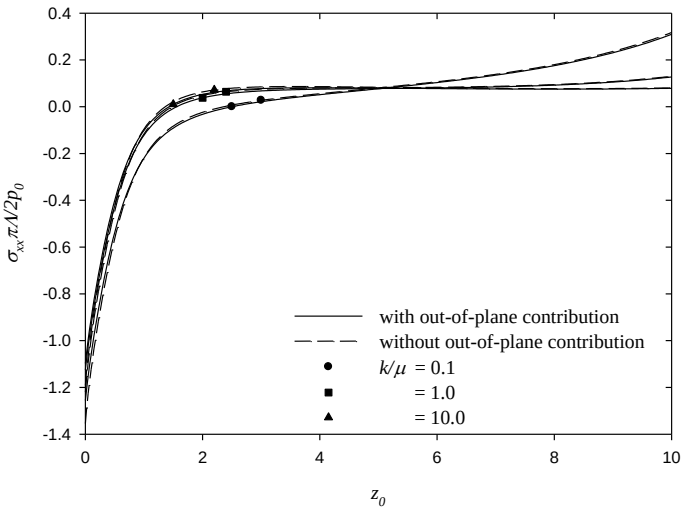

(b) σ_{xx}

Figure 27 Variation of stresses along the *z*-axis for an elastic nanolayer with layer thickness (h_0 = 10) for various values of (k/μ).

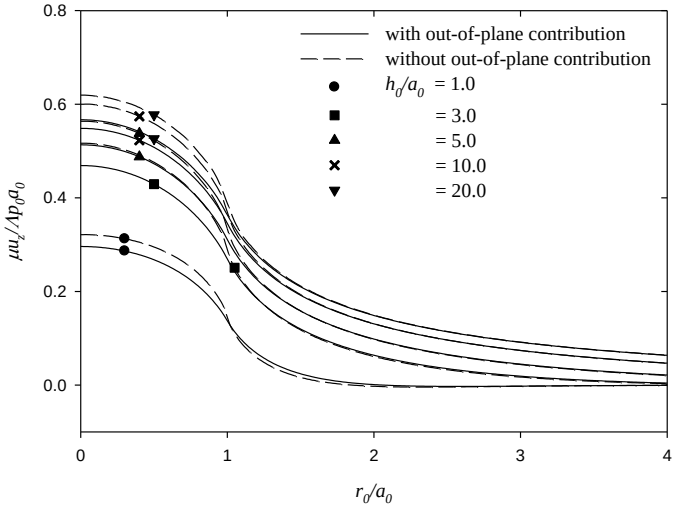

(a) Vertical displacement

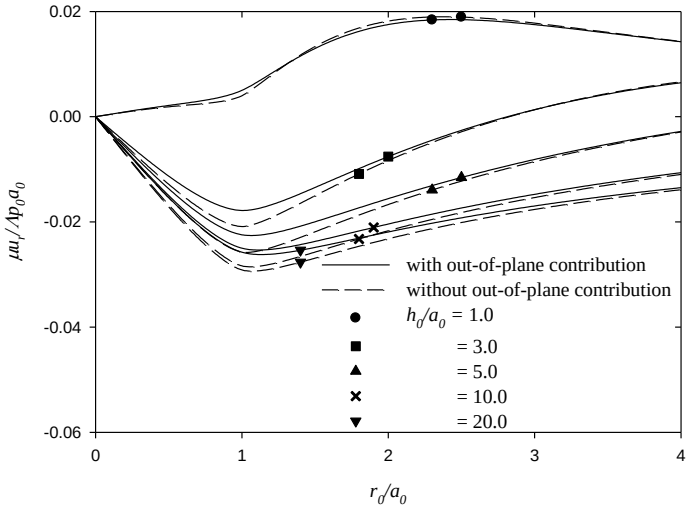

(b) Radial displacement

Figure 28 Displacement profiles along the *r*-axis at the surface of a rigid-based elastic nanolayer with different layer thicknesses.

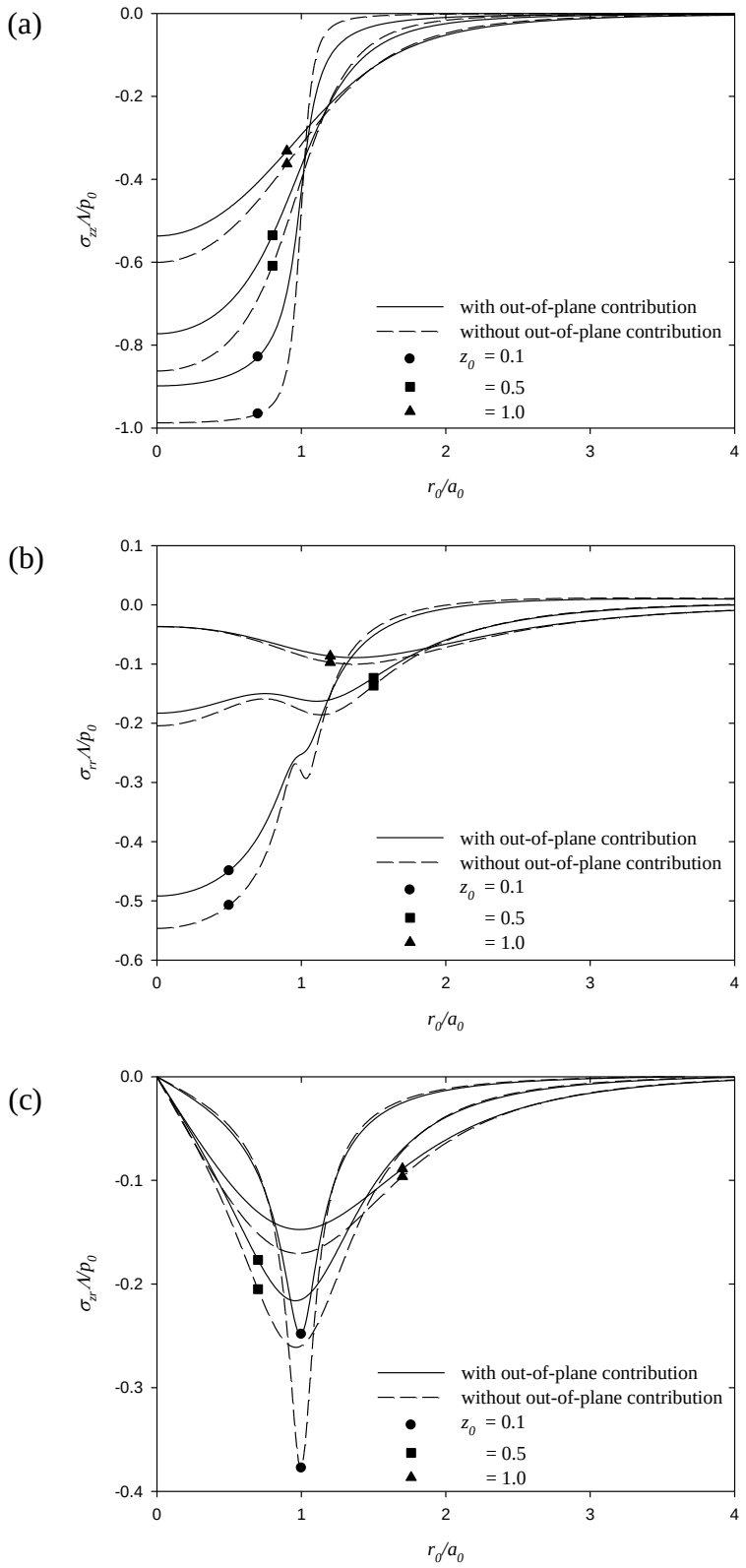

Figure 29 Variation of stresses at various depth z_0 along the r-axis of a rigid-based elastic nanolayer with layer thickness $h_0 / a_0 = 5$.

(d)

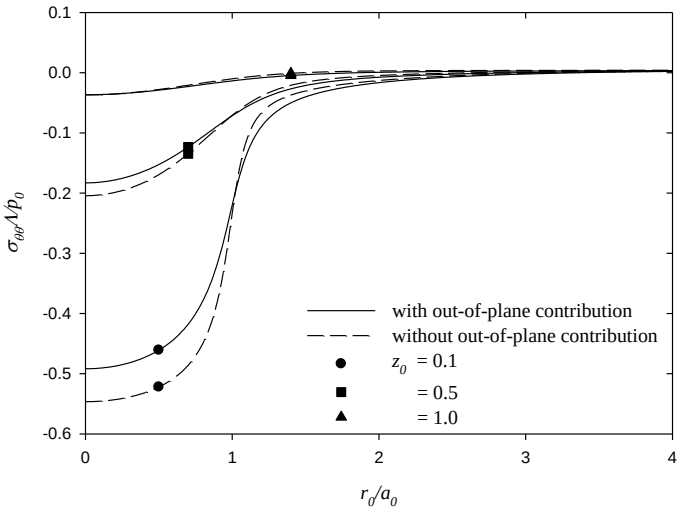

Figure 29 Variation of stresses at various depth z_0 along the *r*-axis of a rigid-based elastic nanolayer with layer thickness h_0 / a_0 = 5 (Continue).

The results for axisymmetry analysis for displacements and stresses of a rigid-based elastic nanolayer under uniformly distributed normal traction are presented in Figures 28 and 29. Results for both vertical and radial displacement along *r*-axis at the surface over the radius loading area a_0 = 1 for various layer thicknesses h_0 are shown in Figure 28. The variation of the normalized vertical and radial displacements in the radial direction are reported in Figures 28(a) and (b) respectively. The vertical displacement profiles for all cases reach the maximum (negative) value at r=0 and decay monotonically and rapidly to zero as r increases. It is evident from the results in Figures 28(a) and (b) that the presence of rigid supporting base significantly lowers the magnitude of the displacement. Normalized stress components plotted along the *r*-axis of a rigid-based elastic nanolayer with h_0 / a_0 = 5 under a uniformly distributed normal traction a_0 = 1 at different depth z_0 = 0.1, 0.5 and 1.0 are presented in Figure 29. It is shown in Figure 29 that the out-of-plane contribution has a notable influence on stress fields especially in the vicinity of the top surface. The influence of the out-of-plane, however, contribution becomes negligible when $r_0 / a_0 > 3$.

Figures 30 and 31 present variations of nondimensional displacements and stresses respectively of an elastic nanolayer under the vertical loading for different values of supporting stiffness (k / μ).The values of all displacements are

substantially reduced as the value of the supporting material stiffness increases. Once again, the influence of the out-of-plane term is clearly observed from the displacement solutions presented in Figure 30. The influence of the supporting stiffness is negligible for vertical and shear stresses whereas for other two stress components, small influence of the supporting stiffness on the near-surface stresses is noted.

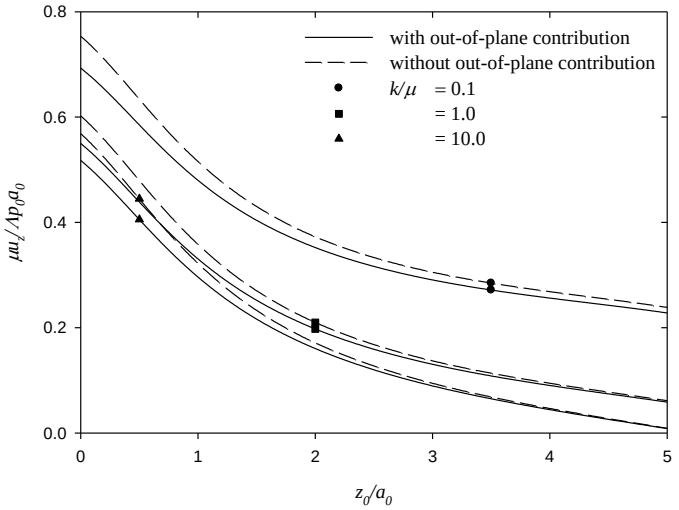

(a) Vertical displacement

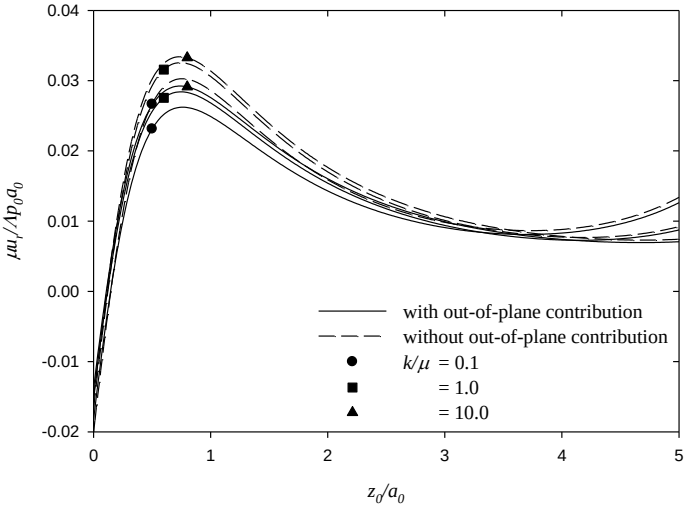

(b) Radial displacement

Figure 30 Displacement profiles at $r_0 / a_0 = 0.5$ along the *z*-axis of an elastic nanolayer with layer thickness $h_0 / a_0 = 5$ for various values of (k / μ).

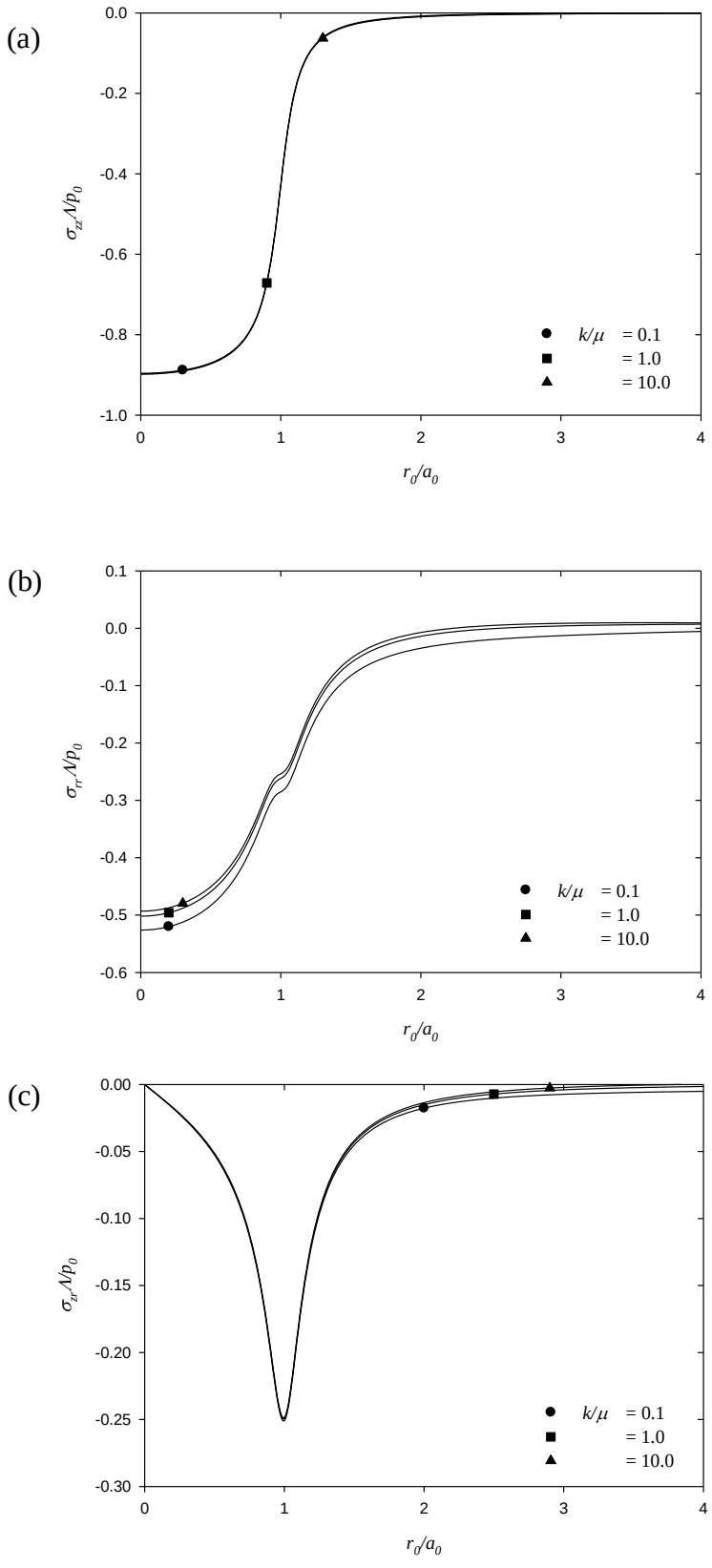

Figure 31 Variation of stresses at depth z_0 = 0.1 along the *r*-axis of an elastic nanolayer with layer thickness h_0 / a_0 = 5 for various values of k / μ.

(d)

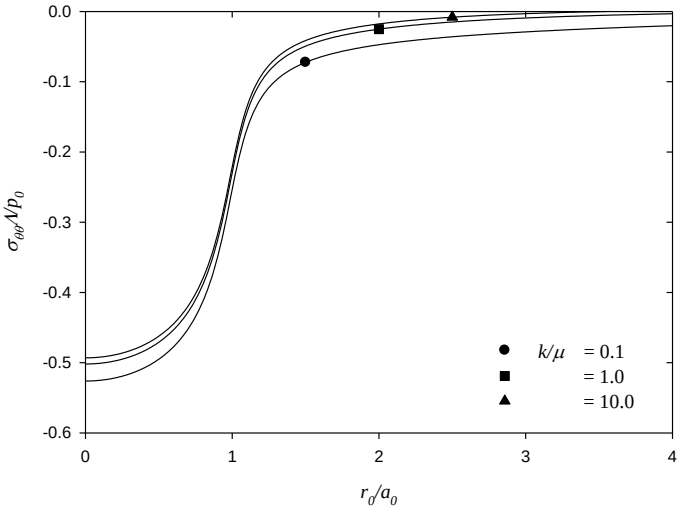

(d) Hoop stress

Figure 31 Variation of stresses at depth z_0 = 0.1 along the *r*-axis of an elastic nanolayer with layer thickness h_0 / a_0 = 5 for various values of k / μ (Continue).

5. Conclusion

The study of nano-scale materials and nanostructures, such as nanoparticles, nanotubes, nanofilms and nanocomposites, which are the key components of nano-scale devices, has important implications in the development of nanotechnology applications. In this study, mechanistic models incorporating surface stress effects are developed and applied to examine the size-dependent behavior of nanofilms on surrounding elastic medium and nano-sized particles reinforced composite materials. A set of analytical techniques for stress and displacement fields corresponding to elastic nanolayer based on Love's representation, Hankel and Fourier integral transforms are adopted to derive explicit integral form solutions for nanolayer problems. A new three-dimensional finite element formulation for analysis of nanoparticle-reinforced composites is developed in the present research project.

Selected numerical results are presented to portray the features of the elastic field responses and properties of elastic materials with nanoscale inhomogeneities. The numerical results presented in this study indicate that the surface stresses have a significant influence on elastic fields of the nanostructures. Stress and material properties for nanocomposite and nanoporous materials show considerable dependence on volume fraction of inhomogeneity. A system of nanofilms-substrate system with the consideration of surface energy effects are stiffer than the corresponding classical plate theory for the case of positive surface stress considered

in the present study. It is also shown in the numerical study that various parameters, namely, modulus of elastic substrate, nanofilm aspect ratio, layer thickness, out-of-plane contribution and surface properties, have a significant influence on the nanofilm-substrate responses. The finite element-based micromechanical model developed in this project provides an efficient tool to analyze and predict the mechanical response of nano-inhomogeneities with arbitrary-shaped nanoscale particles, multiple particles, nanovoid, multiple nanovoid, non-symmetric loading, etc.

6. Output

6.1 International Journal Publication and Manuscript

1. Sapsathiarn Y. and Rajapakse R.K.N.D. (2018) Mechanistic Models for Nanobeams with Surface Stress Effects. *Journal of Engineering Mechanics (ASCE)*, 144(11), 04018098. [Received: April 30, 2018 / Accepted: April 30, 2018 / Published online: August 24, 2018]
https://ascelibrary.org/doi/abs/10.1061/(ASCE)EM.1943-7889.0001520

2. The manuscript "Analysis of nanofilms on elastic substrate with consideration of surface stress effects" by Sapsathiarn Y. and Watthanaprasertkun T., *in preparation*, to be submitted to *Acta Mechanica* in July 2019.

6.2 Others

1. Watthanaprasertkun T. and Sapsathiarn Y. (2018) Mechanistic analysis of nanofilms on elastic substrate with consideration of surface stress effects. The Sixth Asian Conference on Mechanics of Functional Materials and Structures (ACMFMS2018), Tainan, Taiwan, October 26-29, 2018.

2. Chaisuwannakorn S. and Sapsathiarn Y. Finite element based micromechanical model for elastic materials containing nanoscale inhomogeneities. Proceedings of the International Conference on Computational Methods (ICCM2017), Vol.4, 2017, Guilin, Guangxi, China, July 25-29, 2017. http://www.sci-en-tech.com/ICCM2017/PDFs/2692-8356-1-PB.pdf.

References:

Cadek M., Coleman J.N., Ryan K.P., Nicolosi V., Bister G., Fonseca A., Nagy J.B., Szostak K., Béguin F. and Blau W.J. (2004) Reinforcement of polymers with carbon nanotubes: the role of nanotube surface area. Nano Letters, 4(2), pp. 353-356.

Cammarata R.C. (1994) Surface and interface stress effects in thin films. Progress in Surface Science, 46, pp. 1-38.

Cammarata R.C. (1997) Surface and interface stress effects on interfacial and nanostructured materials. Materials Science and Engineering A, 237, 180-184.

Dempsey J.P., Zhao Z.G., Minnetyan L., Li H. Plane contact of an elastic layer supported by a Winkler foundation. Journal of Applied Mechanics. 1990;57:974-80.

Duan H.L, Wang J., Huang Z.P., Karihaloo B.L. (2005) Eshelby formalism for nano-inhomogeneities. Proceedings of the Royal Society A, 461, pp. 3335–3353.

Dym C.L. and Shames I.H. Solid Mechnics. A Variational Approach. McGraw-Hill, 1973.

Eshelby J.D. (1957) The determination of the elastic field of an ellipsoidal inclusion and related problems. Proceedings of the Royal Society A, 241, pp. 376–396.

Fischer F.D., Waitz T., Vollath D. and Simha N.K. (2008) On the role of surface energy and surface stress in phase-transforming nanoparticles. Progress in Materials Science, 53, pp. 481-527.

Gao Y.F., Xu H.T., Oliver W.C. and Pharr G.M. (2008) Effective elastic modulus of film-on-substrate systems under normal and tangential contact. Journal of the Mechanics and Physics of Solids, 56(2), pp. 402-416.

Gradshteyn I.S., Ryzhik I.M. Table of integrals, series, and products. San Diego, CA: Academic; 2000.Gurtin M.E. and Murdoch A.I. (1975) A continuum theory of elastic material surfaces. Archive for Rational Mechanics and Analysis, 57, pp. 291–323.

Gurtin M.E. and Murdoch A.I. (1978) Surface stress in solids," International Journal of Solids and Structures, 14, pp. 431–440.

Gurtin M.E. (1998) A general theory of curved deformable interfaces in solids at equilibrium. Philosophical Magazine A, 78, pp. 1093-1109.

Jammes M., Mogilevskaya S.G. and Crouch S.L. (2009) Multiple circular nanoinhomogeneities and/or nano-pores in one of two joined isotropic elastic halfplanes. Engineering Analysis with Boundary Elements, 33, pp. 233–248.

Lee B. and Rudd R.E. (2007) First-principles study of the Young's modulus of Si <001> nanowires. Physical Review B, 75, pp. 041305(R).

Lim C.W. and He L.H. (2004) Size-dependent nonlinear response of thin elastic films with nano-scale thickness. International Journal of Mechanical Sciences, 46, pp. 1715–1726.

Liu C. and Rajapakse R.K.N.D. (2013) A Size-dependent continuum model for nanoscale circular plates. IEEE Transactions on Nanotechnology, 12(1), pp. 13–20.

Lu P., He L.H., Lee H. P. and Lu C. (2006) Thin plate theory including surface effects. International Journal of Solids and Structures, 43, pp. 4631–4647.

Lucas B.N., Hay J.C. and Oliver W.C. (2004) Using multidimensional contact mechanics experiments to measure Poisson's ratio. Journal of Materials Research, 19(1), pp. 58-65.

Marko K. and Preziosi L. Heterogeneous media: Micromechanics modeling methods and simulations, Birkhauser Verlag, Switzerland, 2000.

Miller R.E. and Shenoy V.B. (2000) Size-dependent elastic properties of structural elements. Nanotechnology, 11(3), pp. 139–147.

Mogilevskaya S.G., Crouch S.L. and Stolarski H.K. (2008) Multiple interacting circular nano-inhomogeneities with surface/interface effects. Journal of the Mechanics and Physics of Solids, 56, pp. 2298–2327.

Murr L.E. Interfacial Phenomena in Metals and Alloys. Addison-Wesley, London, 1975.

Nemat-Nasser S. and Hori M. Micromechanics: Overall properties of Heterogeneous solids, Elsevier, New York, 1999.

Oliver W.C. and Pharr G.M. (1992) Improved technique for determining hardness and elastic modulus using load and displacement sensing indentation experiments. Journal of Materials Research, 7(6) pp. 1564-1583.

Orowan E. (1970) Surface energy and surface tension in solids and liquids. Proceedings of the Royal Society of London A, 316, pp. 473–491.

Poncharal P., Wang Z.L., Ugarte D. and de Heer W.A. (1999) Electrostatic deflections and electromechanical resonances of carbon nanotubes. Science, 283, pp. 1513-1516.

Poulos H. G. (1967) Stresses and Displacements in an elastic layer underlain by a rough rigid base. Geotechnique, 17(4), pp. 378-410.

Povstenko Y.Z. (1993) Theoretical investigation of phenomena caused by heterogeneous surface tension in solids. Journal of the Mechanics and Physics of Solids, 41, pp. 1499-1514.

Sapsathiarn Y. and Rajapakse R.K.N.D. (2013) Finite-element modeling of circular nanoplates. Journal of Nanomechanics and Micromechanics-ASCE, 3(3), pp. 59–66.

Sapsathiarn Y. and Rajapakse R.K.N.D. (2014) Finite-element modeling of circular nanoplates, ASCE Journal of Micromechanics and Nanomechanics, 3 (3), pp. 59-66.

Sapsathiarn Y. and Rajapakse R.K.N.D. (2016) Static and dynamic analyses of nanoscale rectangular plates incorporating surface energy. Acta Mechanica, pp. 1-15.

Sapsathiarn Y. and Rajapakse R.K.N.D. (2018) Mechanistic Models for Nanobeams with Surface Stress Effects. Journal of Engineering Mechanics (ASCE), 144(11), pp. 04018098.

Sharma P. and Ganti S. (2004) Size-dependent Eshelby's tensor for embedded nano-inclusions incorporating surface/interface energies. Journal of Applied Mechanics, 71(5), pp. 663-671.

Shenoy V.B. (2005) Atomistic Calculations of Elastic Properties of Metallic Fcc Crystal Surfaces. Physical Review B, 71(9), pp. 094104.

Shuttleworth R. (1950) The surface tension of solids. Proceedings of the Physical Society Section A, 63, pp. 444-457.

Singh R.P., Zhang M. and Chan D. (2002) Toughening of a brittle thermosetting polymer: effects of reinforcement particle size and volume fraction. Journal of Materials Science, 37(4), pp. 781-788.

Sneddon I.N. Fourier transform. New York: McGraw-Hill; 1951.Tian L. and Rajapakse R.K.N.D. (2007) Analytical solution for size-dependent elastic field of a nanoscale circular inhomogeneity. ASME Journal of Applied Mechanics, 74, pp. 568–574.

Wong E.W., Sheehan P.E. and Lieber C.M. (1997) Nanobeam mechanics: Elasticity, strength, and toughness of nanorods and nanotubes. Science, 277, pp. 1971–1975.

Yakobson B.I. Nanomechanics, Handbook of Nanoscience, Engineering and Technology, William A.G., Donald W.B., Sergey E.L., and Gerard J.L., eds., CRC, Boca Raton, FL, 2003.

Zhao X.J., Rajapakse R.K.N.D. Analytical solutions for a surface-loaded isotropic elastic layer with surface energy efects. International Journal of Engineering Science. 2009;47:1433-44

Zienkiewicz O.C. and Taylor R.L. The Finite Element Method, Butterworth-Heinemann, Boston, 2000.